

# 1 Highlights

## 2 **A Large-scale Neurocomputational Model of Spatial Cognition Integrating Memory with Vision**

3 Micha Burkhardt, Julia Bergelt, Lorenz Gönner, Helge Ülo Dinkelbach, Frederik Beuth, Alex Schwarz, Andrej

4 Bicanski, Neil Burgess, Fred H. Hamker

- 5 • Novel, systems-level approach integrates vision and spatial memory/imagery
- 6 • Integration of multiple brain areas gives rise to key aspects of spatial cognition
- 7 • Interfacing memory and vision through parietal areas improves object localisation
- 8 • Virtual environment opens up new options for the assessment of computational models

9 A Large-scale Neurocomputational Model of Spatial Cognition Integrating  
10 Memory with Vision

11 Micha Burkhardt<sup>a,1,2</sup>, Julia Bergelt<sup>a,1,2</sup>, Lorenz Gönner<sup>b,c,1,2</sup>, Helge Ülo Dinkelbach<sup>a,1,2</sup>, Frederik Beuth<sup>a,1,2</sup>,  
12 Alex Schwarz<sup>a,1,2</sup>, Andrej Bicanski<sup>d,1,2</sup>, Neil Burgess<sup>e,2</sup>, Fred H. Hamker<sup>a,2,\*</sup>

<sup>a</sup>Chemnitz University of Technology, 09107, Chemnitz, Germany

<sup>b</sup>Technische Universität Dresden, Faculty of Psychology, 01062, Dresden, Germany

<sup>c</sup>Technische Universität Dresden, Department of Psychiatry, 01307, Dresden, Germany

<sup>d</sup>Newcastle University, NE1 7RU, Newcastle upon Tyne, United Kingdom

<sup>e</sup>University College London, WC1E 6BT, London, United Kingdom

---

13 **Abstract**

We introduce a large-scale neurocomputational model of spatial cognition called 'Spacecog', which integrates recent findings from mechanistic models of visual and spatial perception. As a high-level cognitive ability, spatial cognition requires the processing of behaviourally relevant features in complex environments and, importantly, the updating of this information during processes of eye and body movement. The Spacecog model achieves this by interfacing spatial memory and imagery with mechanisms of object localisation, saccade execution, and attention through coordinate transformations in parietal areas of the brain. We evaluate the model in a realistic virtual environment where our neurocognitive model steers an agent to perform complex visuospatial tasks. Our modelling approach opens up new possibilities in the assessment of neuropsychological data and human spatial cognition.

14 *Keywords:* brain-inspired neural networks, spatial reference transformation, parietal cortex, visual attention,  
15 spatial memory and imagery

---

---

\*Corresponding author

<sup>1</sup>Equal contribution

<sup>2</sup>E-mail addresses:

micha.burkhardt@informatik.tu-chemnitz.de (Micha Burkhardt)

julia.bergelt@informatik.tu-chemnitz.de (Julia Bergelt)

lorenz.goenner@tu-dresden.de (Lorenz Gönner)

helge-uelo.dinkelbach@informatik.tu-chemnitz.de (Helge Ülo Dinkelbach)

frederik.beuth@informatik.tu-chemnitz.de (Frederik Beuth)

alex.schwarz@informatik.tu-chemnitz.de (Alex Schwarz)

andrej.bicanski@newcastle.ac.uk (Andrej Bicanski)

n.burgess@ucl.ac.uk (Neil Burgess)

fred.hamker@informatik.tu-chemnitz.de (Fred H. Hamker)

## 16 1. Introduction

17       Uncovering the underlying mechanisms of spatial cognition involves a broad spectrum of research ranging  
18 from experimental studies with animals and humans to neurocomputational modelling. Spatial cognition in  
19 its broadest interpretation must solve various problems including object detection (Cavanagh, 2011), visual  
20 attention (Carrasco, 2011), eye- and body-movements (Land, 2009), as well as spatial memory and navigation  
21 (Burgess, 2008). This combination of tasks requires an intimate coupling between visual perception and  
22 cognition as outlined in the seminal work of Ballard et al. (1997), which suggests a variable binding of  
23 objects in the world to internal cognitive programs through deictic ("do-it-where-I'm-looking") strategies.  
24 In visuospatial tasks, the issue of spatial reference frames also comes into play: While visual information is  
25 initially processed in a retinal reference frame, grasping often relies on body or limb centred reference frames  
26 (Pouget & Sejnowski, 1997), and navigation can even recruit world-centred (allocentric) reference frames  
27 (Avraamides & Kelly, 2008).

28       We propose that integrating mechanistic models into larger scale cognitive system models is required to  
29 explain such high-level cognitive functions. An example of this in a related domain is the Spaun architecture  
30 (Eliasmith et al., 2012), which implements a large-scale spiking network to output physical movements of  
31 a virtual robotic arm in a versatile set of cognitive tasks like digit recognition, serial working memory, or  
32 mental arithmetic. In the context of spatial cognition, previous bio-inspired models mostly focus on spatial  
33 navigation (Becker & Burgess, 2000; Byrne et al., 2007) and a few modelling approaches also exist in the field  
34 of bio-inspired robots, although with varying biological plausibility (Antonelli et al., 2014; Moulin-Frier et al.,  
35 2018). **As overt behavior is typically the result of a coordinated activation involving many parts of the brain,**  
36 **attempts are required to not only integrate models, but also to improve the understanding of function across**  
37 **brain parts, which is limited when neurocomputational models are only studied in isolation.**

38       **A particular aspect we are interested in is the ability of humans to guide attention by long-term memory.**  
39 **Experimental studies have revealed that the hippocampus, via the parietal cortex, contributes to object**  
40 **detection (Summerfield et al., 2006; Salsano et al., 2021). However, most experimental studies and computa-**  
41 **tional models that study attention and vision typically direct attention based on visual cues, but not based**  
42 **on long-term memory.** From a conceptual point of view, the necessity for such an interaction **of vision and**  
43 **memory** has previously been outlined by Epstein et al. (2017), who argued that an effective use of a cognitive  
44 map requires to anchor such a map to the world. To the best of our knowledge, this interplay of memory and  
45 vision in a spatial context is yet to be explored by neurocomputational models.

46       In order to explore this interaction, we introduce the Spacecog model as a systems-level approach to  
47 spatial cognition and shed light on how multiple brain areas might interact with each other to display key  
48 elements of spatial memory and object detection. Built on the foundation of previous work done under  
49 the European research project "Spatial Cognition" (Hamker, 2015), Spacecog builds upon three individual  
50 neurocomputational models: A model of attention including object recognition and object detection (Beuth,

51 2019), a model of perisaccadic space perception (Bergelt & Hamker, 2019), and a model of spatial memory  
52 and imagery (Bicanski & Burgess, 2018). Through this integration, we propose how parietal cortical areas  
53 could interface with visual and **long-term memory** areas to form a complex understanding of the surrounding  
54 environment. **As visual information is initially encoded in a retinocentric reference frame the question arises**  
55 **how spatial memory, stored in a world-centered reference frame, can guide visual perception.**

56 The individual parts of the Spacecog model are anatomically constrained and, as shown by the original  
57 publications, replicate experimental findings of neural mechanisms responsible for vision, attention, eye  
58 movements, and memory recall. By combining them into a large-scale neurocomputational model of spatial  
59 cognition, we aim to bridge the gap between previously disparate lines of research and particularly explore  
60 the putative role of the parietal cortex interfacing vision and memory. Acting as a case study for an increased  
61 understanding of the integration of brain areas, we propose how the brain deals with complex tasks in our  
62 everyday environment. We test the model on a functional level in a real-world like virtual environment, in  
63 which a neuro-cognitive agent has the task to successfully locate, encode, recall and re-localise objects in a  
64 realistic scene.

## 65 **2. Methods**

66 The neurocomputational model has been used to perform visuospatial computations for a neuro-cognitive  
67 agent (Figure 1a) which operates in a virtual environment (Figure 1b). We next introduce the virtual  
68 environment and explain the model and its functions.

### 69 *2.1. Virtual Environment*

70 The Unity game engine<sup>3</sup> was used to create the spatial environment (a child’s room) and a cognitive  
71 agent, which we will refer to as Felice. Felice is connected to the neural network through a custom network  
72 interface built with Google’s protocol buffers<sup>4</sup>. This extra step allows for the computational network to  
73 run on a separate Linux server, while Unity is running on a Windows computer, distributing the workload.  
74 Alternatively, it is possible to use virtualisation techniques (e.g. the Windows Subsystem for Linux, WSL2) to  
75 run the whole model on a single machine.

76 Pictured in Figure 1b;c, the main feature of the environment is a large desk with several toys placed on  
77 top, which can be recognised, remembered, and recalled by Felice. During simulations, Felice is externally  
78 instructed to walk into the vicinity of a random target object, which is placed among others on her desk. She  
79 first localises and encodes this object into memory, and is then instructed to walk to a different location.  
80 Once arrived, Felice will use object identity to recall information about the object location from memory.  
81 This subsequently allows Felice to walk back to the original position and to visually re-localise the object.

---

<sup>3</sup><https://unity.com/>

<sup>4</sup><https://developers.google.com/protocol-buffers>

82 By default, objects in the virtual environment are subject to a perspectival projection, which results from  
 83 a 3D world being projected onto a 2D camera plane. This projection, however, results in artefacts of distorted  
 84 proportions of objects, especially in the corners of an image. **While the model can tolerate small deformations**  
 85 **and still performs well in such cases, we mitigate any potential issues by introducing a spherical projection**  
 86 **shader to more closely mimic human vision and to ensure position-invariant object proportions in the visual**  
 87 **field (Figure 1c).**

88 The visual, perceptual input from the virtual environment (as 408x308p colour images) is processed by  
 89 the computational model, which returns commands for specific motor actions like positional changes (rotation  
 90 and translation) or eye movements. Therefore, Felice can perceive objects from different angles and distances,  
 91 as well as under different lighting. This creates a challenging, real-world-like environment for her to act in.

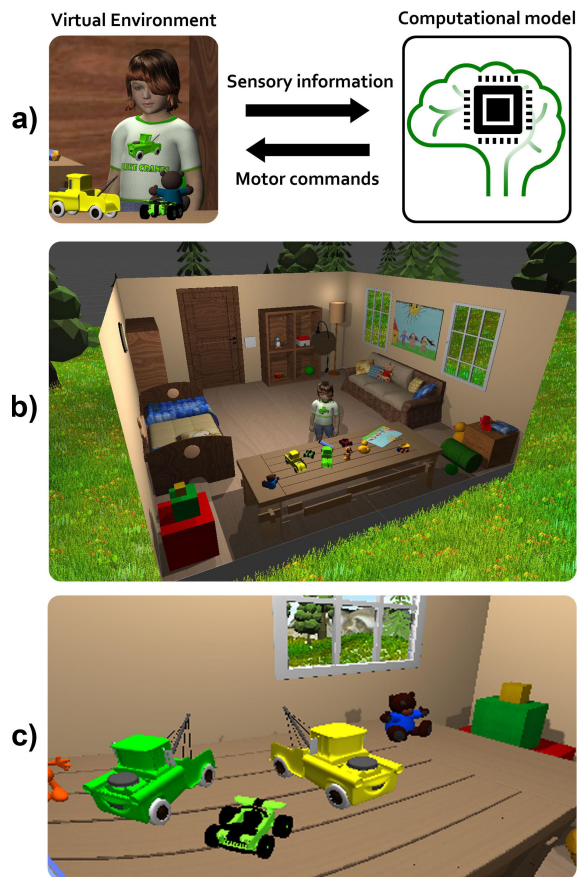


Figure 1: The virtual environment. a) The virtual environment provides sensory information which is sent to the model. The neural network then evaluates these data to form an internal, dynamic representation of the environment and outputs motor commands to be performed by the agent. b) The child's room of the cognitive agent called Felice. She is able to navigate and shift gaze as well as locate, remember, and recall multiple objects in this environment. c) Example of a visual image from the viewpoint of the agent. For simplicity, we do not model different resolutions of an object with respect to **retinal** eccentricity and also only use monocular vision (single eye camera).



93 Spatial cognition is a large field of research. We here specifically aim to address the interplay of visuospatial  
94 and memory components. This requires an integration of object memory with visual perception including  
95 eye-centred visual processes, world-centred information of objects and space in long-term memory, as well as  
96 visual attention and object detection. For this, three individual models are integrated to form a large-scale  
97 neurocomputational model (Figure 2). These biologically rooted models were previously described in detail  
98 and have been extensively validated and compared with human and macaque experimental data. Even though  
99 some of these data are from different species, the model can be considered being a generic model of processes  
100 that are likely similar among different species.

101 Our integrated model can operate in two directions corresponding to processes of encoding and mental  
102 imagery: 1) In encoding processes, an object is searched by the agent via means of feature-based attention  
103 which alters the response profile of object cells in area V4/IT of the visual cortex. At the same time, this  
104 V4/IT information drives the frontal eye fields (FEF) for saccade target selection. Spatial information about  
105 this object is transformed from an eye-centred reference frame into a head-centred reference frame via the  
106 lateral intraparietal cortex (LIP) and, after being combined with environmental information in the parietal  
107 window (PW), transformed into a world-centred reference frame via the retrosplenial transformation circuit  
108 (RSC/TR). For long-term memory storage, this combined information of objects and space is encoded in an  
109 attractor network in the medial temporal lobe (MTL). 2) In processes of mental imagery, neural patterns  
110 from a previous encoding phase are re-instated in MTL by a cue-based memory retrieval using object identity.  
111 The retrieved patterns contain spatial information of the object and agent during encoding (their relative  
112 location to each other and their absolute locations relative to the environment). They are used for spatial  
113 navigation (here only the navigational goal) and furthermore transformed from world-centred into eye-centred  
114 reference frames via RSC and LIP for attentional control in FEF.

### 115 *2.2.1. Object Recognition*

116 To implement the capability of recognising and localising objects, the visual part of the computational  
117 model incorporates key elements of the ventral stream in the primate brain (Beuth, 2019). The input to the  
118 model is the agent’s current visual field, which is a monocular RGB-image. Only daylight vision is considered,  
119 which in primates is represented by L,M, and S cones in the retina to process long (L), middle (M) and short  
120 (S) wavelengths of the visible light spectrum. For this purpose, the image is processed in area V1, which  
121 includes neurons organised in three channels. These channels are arranged in a retinotopic fashion and include  
122 cells for the red-green (L-M) and blue-yellow (LM-S) colour contrasts which are commonly found in the lateral  
123 geniculate nucleus (LGN) (Gegenfurtner & Kiper, 2003). In addition, the channels contain oriented edges  
124 which are derived from the image using Gabor filters (Jones & Palmer, 1987). Thus, they represent neurons  
125 with receptive fields commonly found in primary visual cortex (V1) simple cells (Jones & Palmer, 1987). The  
126 low level colour and orientation features within the field of view are then fed into higher visual areas for  
127 further processing (Figure 2, red parts).

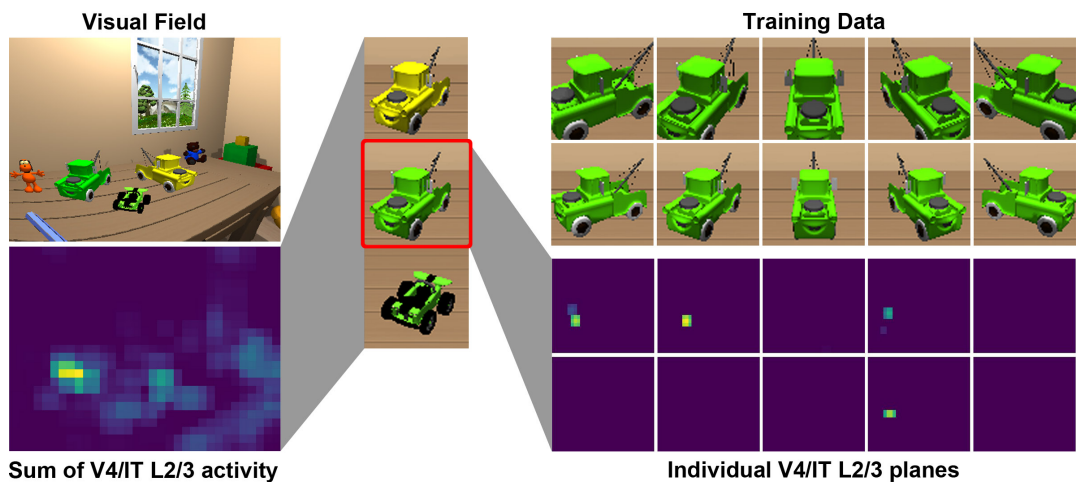


Figure 3: Object localisation for the green crane. Area V4/IT L2/3 consists of 30 neuronal layers/planes. Each plane encodes cells representing an object from a particular view-point (view-tuned cells). The number of planes is a result of the training procedure, as for each of the three objects weights were calculated for five different rotations and two sizes (here shown for the green crane). Thus, for each object we only use 10 images for training. The sum of neuronal activity in V4/IT L2/3 over all planes/objects (left) as well as activity in the individual planes for the green crane (right) are shown. When the agent is searching for the green crane (denoted by the red square), these planes are subject to feature-based attention from the prefrontal cortex. Their neural activity reflects the match of parts of the encoded object with the particular visual image, and the gain via feature-based attention.

128 Object recognition requires more narrowly tuned cells that respond selectively to an object or parts of it.  
 129 Hence, V1 features need to be combined in higher visual areas by learning useful representations of objects.  
 130 In our model, we simulate a higher visual area (V4/IT; Figure 2), representing high-level visual cortices  
 131 such as the fourth visual cortex (V4) or the inferior temporal cortex (IT), with cells encoding object views  
 132 (object-view tuned cells) as found in the inferior temporal cortex (Logothetis et al., 1995). V4/IT Layer 4  
 133 (V4/IT L4) encodes these object views, which are created by a convolution of the activities of V1 neurons with  
 134 pre-learned weights. These weights were generated through a process called one-shot learning (Jamalian et al.,  
 135 2016), which generated the weight matrix directly from the output of V1 complex cells in a prior learning  
 136 phase. For training, only 10 images per object (five rotations, two sizes) were used to allow for some degree of  
 137 invariant recognition. Furthermore, spatial pooling of these activities takes place in V4/IT Layer 2/3 (V4/IT  
 138 L2/3). Like Layer 4, Layer 2/3 neurons have still a spatial organisation being selective for different parts of  
 139 the image (Figure 3). Layer 2/3 neurons are subject to feature-based attention from the prefrontal cortex  
 140 (PFC), enhancing the gain of neurons that respond to the target object.

141 This object recognition part is comparatively simple compared to deep neural networks. Thus, our emphasis  
 142 is not on recognising a large number of objects, but to allow object recognition on a number of pre-selected  
 143 objects with only a very small amount of training data (Figure 3). Technically, as further processing in  
 144 the network is not dependent on the specific structure of the V1-V4/IT path, one could replace the image  
 145 processing by a deep neural network to provide our model with a feedforward input into V4/IT L4, as we did



146 not implement feedback connections back to V1.

### 147 *2.2.2. Saccade Execution*

148 Activities of object neurons in V4/IT L2/3 are pooled over objects to elicit spatially distributed neural  
149 activations in the frontal eye fields (FEF; Figure 2, yellow parts). Neural populations in FEF are responsible  
150 for the processing of spatial information and the preparation of eye-movements, particularly saccade target  
151 selection. This part is based on a model developed by Zirnsak et al. (2011).

152 Our model of the FEF is divided into three parts, namely FEF-visual (FEFv), FEF-visuomovement  
153 (FEFvm) and FEF-movement (FEFm), inspired by recordings from frontal eye-field neurons (Schall et al.,  
154 2004). From a functional perspective, FEFv indicates potentially relevant locations by taking the maximum  
155 activities over features in V4/IT L2/3. Feedforward soft-competition, combined with feedback from eye  
156 movement preparation in FEFm, activates FEFvm neurons. Feedforward projections from FEFvm to FEFm  
157 accompanied by strong lateral competitive interactions lead to the potential target of the upcoming saccade.  
158 If FEFm neurons increase their activation beyond a threshold, a saccade is executed towards the centre of  
159 gravity of the activation profile at that time. Given the saccade target, the actual movement of the eyes is  
160 then modelled by an extended version of the saccade generator of Van Wetter & Van Opstal (2008).

### 161 *2.2.3. Attention*

162 Among other tasks, our model is designed to perform object localisation supported by attentive dynamics,  
163 most notably feature-based and spatial attention. This model component is based on previous models  
164 that explain attention as an emergent result of neural dynamics, rather than postulating brain circuits that  
165 exclusively compute attention (Hamker, 2003, 2005b; Zirnsak et al., 2011) and is inspired by biased competition  
166 (Desimone & Duncan, 1995) and feature-similarity (Treue, 2001) frameworks of attention. The present model  
167 is built upon a microcircuit of attention proposed by Beuth & Hamker (2015), who compared and fitted their  
168 model to electrophysiological data of more than 10 different experiments that studied the mutual influence  
169 of stimuli placed within or near receptive fields in different states of attention. This is to date the most  
170 exhaustive comparison of a model with data recorded from neurons localised in different visual brain areas  
171 modulated by attention.

172 A top-down signal from PFC amplifies target-feature-specific activities in area V4/IT, independent of the  
173 location or size of features in the visual field and allows the selection of specific objects (Beuth, 2019). This  
174 can be seen in the sum of V4/IT L2/3 activity in Figure 3, where feature-based attention amplifies features  
175 of the green crane. In parallel, spatial attention emerges by feedback from FEFvm cells, which link spatial  
176 attention to the eye movement plan (Hamker et al., 2008) and can also account for attentional capture, based  
177 on the attention-related N2pc component of EEG recordings (Novin et al., 2021).

178 The here presented integrated model extends spatial attention with an additional loop between FEF and  
179 LIP. This extension by the LIP circuit is crucial for aspects of spatial cognition as LIP connects visual areas

180 through parietal areas with MTL, where long-term information of objects and the environment are stored. If  
181 this information is recalled, LIP can, through coordinate transformations which are more closely described in  
182 the next section, generate an additional spatial attention signal to recalled locations of previously encountered  
183 and encoded objects. As this attentional signal does not require a feature-search in the entire visual field,  
184 it acts faster than spatial attention generated in the V4/IT-FEF loop. Also, this spatial attention signal is  
185 updated during eye movements to ensure that attention is directed to an object in space regardless of gaze  
186 position.

187 The general role of the LIP circuit in spatial attention has previously been motivated by Bisley & Goldberg  
188 (2003) and Goldberg et al. (2006). The computational model of spatial updating in the parietal cortex was first  
189 introduced by Ziesche & Hamker (2011) and later extended by Ziesche & Hamker (2014); Bergelt & Hamker  
190 (2016); Jamalian et al. (2017); Ziesche et al. (2017); Bergelt & Hamker (2019). The model has been compared  
191 to and motivated by studies exploring predictive remapping of attention (Rolfs et al., 2010), lingering of  
192 attention after saccades (Golomb et al., 2010), a combination of both (Jonikaitis et al., 2013), perisaccadic  
193 mislocalisation of briefly flashed stimuli (Van Wetter & Van Opstal, 2008), and saccadic suppression of  
194 displacement (Deubel et al., 1996).

#### 195 *2.2.4. Coordinate Transformation*

196 Spatial tasks of embodied agents operating in, and interacting with the world require coordinate transfor-  
197 mations between different reference frames. Generally speaking, we can distinguish between egocentric and  
198 allocentric (world-centred) reference frames. Egocentric reference frames include eye-centred or head-centred  
199 reference frames, while allocentric reference frames could relate to cardinal directions or visual landmarks. In  
200 our case, visual information about an object, initially processed in an eye-centred reference frame, could then  
201 be transformed into an allocentric reference frame for storage in long-term memory. It has been proposed that  
202 gain fields and radial basis functions (Figure 4) can perform these coordinate transformations between eye-  
203 and head-centred reference frames (Pouget & Sejnowski, 1997; Pouget et al., 2002), and diagonal connection  
204 patterns for this transformation have recently been observed in *Drosophila* (Lu et al., 2022). In our model,  
205 these coordinate transformations are performed in LIP (Ziesche & Hamker, 2011; Bergelt & Hamker, 2019)  
206 and RSC (Bicanski & Burgess, 2018) (Figure 2, green parts).

207 While the agent is searching for an object, retinal (eye-centred) input from area V4/IT is passed to  
208 LIP, along with a retinotopic spatial signal from FEF, a proprioceptive eye position (EP) signal encoding  
209 the eye position in a head-centred reference frame, and a corollary discharge (CD) signal encoding the eye  
210 displacement in an eye-centred reference frame. According to Ziesche & Hamker (2011) and Bergelt & Hamker  
211 (2019), the retinal signal from V4/IT L2/3 is fed into LIP maps, where it is gain-modulated by the CD signal  
212 (LIP CD) as well as the EP signal (LIP EP). This produces a combined representation of eye position and  
213 object position. Reading out the activity in LIP, we receive the perceived spatial position of an object in  
214 head-centred coordinates stored in  $X_h$  (Figure 4;  $\text{Stim}_{\text{head}}$ ). As mentioned above, this process can also be

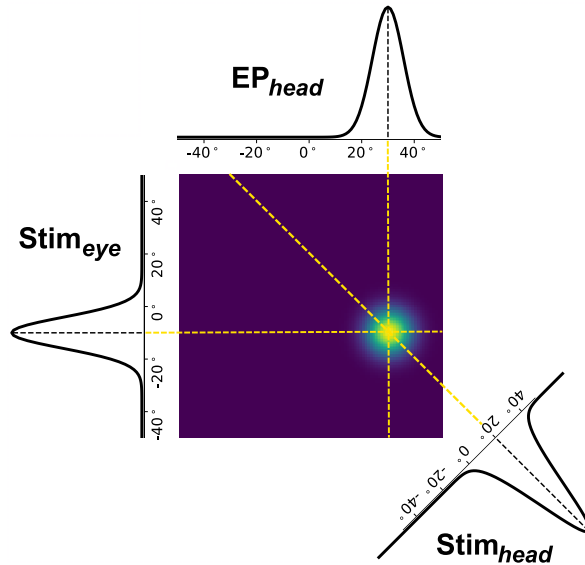


Figure 4: Coordinate transformation in a radial basis function network. In this example, a stimulus position in an eye-centred reference frame gets transformed into a head-centred reference frame. The eye fixates on a position at  $30^\circ$  ( $EP_{\text{head}}$ ) and the eye-centred stimulus position is at  $-10^\circ$  ( $Stim_{\text{eye}}$ ). Thus, the resulting head-centred position of the stimulus is at  $20^\circ$  ( $Stim_{\text{head}}$ ). Further, planned gaze shifts (and not only eye position) are also used for coordinate transformation. The same principle is also used for transformations between head- and world-centred reference frames. Importantly, this transformation can also be performed in the opposite direction (world-centred to head-centred or head-centred to eye-centred).

215 performed in a top-down fashion to transform a head-centred signal into an eye-centred signal, which is sent  
 216 to FEFv to attend to the retinotopic position of a previously encoded object.

217 Object location information and the local environmental layout need to be combined with head direction to  
 218 enable an unambiguous representation of objects and space. This is conducted in the spatial memory pathway  
 219 of the model (Bicanski & Burgess, 2018), which demonstrates how neural representations of head-centred  
 220 (egocentric) experiences interface with world-centred representations in long-term memory. The parietal areas  
 221 of the brain, which we call 'parietal window' (PW), include head-centred representations of discrete objects  
 222 (PWo) and boundaries (PWb). Here, objects refer to the three potential target objects and boundaries refer  
 223 to the four walls of the room.

224 In addition to object information (PWo), during encoding/perception, the parietal window is also driven  
 225 by high-level (head-centred) visual information of boundaries (PWb). This input is externally provided by  
 226 the virtual environment and not explicitly modelled. The resulting activities in PW are fed into RSC, where  
 227 the head direction signal (HD) provides gain-modulation to transform the egocentric representations into  
 228 a world-centred reference frame, similar to related mechanisms proposed for the posterior parietal cortex  
 229 (Pouget & Sejnowski, 1997; Whitlock et al., 2008). This circuit can also further be used in the opposite  
 230 direction, which is required for processes of recall. World-centred information about boundaries and objects  
 231 stored in MTL are then transformed back into a head-centred reference frame in PW via RSC.

### 232 2.2.5. Spatial Memory and Imagery

233 After visuospatial information is transformed into a world-centred reference frame through RSC, the  
234 resulting allocentric representations located in the medial temporal lobe (MTL; Figure 2, blue parts) can  
235 contribute to long-term memory (Bicanski & Burgess, 2018). Information in MTL consists of boundary  
236 information, which is encoded in so called boundary vector cells (BVCs) for the external boundaries of the  
237 environment (as an allocentric counterpart of PWb cells) and object vector cells (OVCs), which encode the  
238 position of objects and hippocampal place cells (PCs), which encode an allocentric position of the agent in  
239 space (see Bicanski & Burgess (2020) for a more in-depth review of the properties of vector coding cells in the  
240 brain). For a given spatial position encoded by PCs, an explicit subset of BVCs and OVCs are co-active to form  
241 a high-level representation of the spatial scene. By connecting co-active populations via Hebbian-like learning,  
242 an allocentric MTL attractor network is formed, which enables spatial long-term memory. Additionally,  
243 since BVCs and OVCs do not distinguish between specific boundaries and objects, perirhinal neurons (PR),  
244 high-level neurons of the ventral stream, code for the identity of boundaries (PRb) and objects (PRo). These  
245 allocentric representations can subsequently be used for memory recall. Cueing a previously encoded object in  
246 MTL enables the re-instated neuronal activities to drive the transformation circuit in the opposite direction,  
247 establishing egocentric representations to be reconstructed from memory and thus enabling spatial imagery  
248 through the parietal window. This egocentric information can then further be used as attentional input for  
249 LIP and FEF.

250 The basis of stable representations of self-location is the agent’s perception of boundaries, which drives  
251 firing of BVCs. Their activity, in turn, activates corresponding place cell firing, in a manner consistent with  
252 empirical data (O’Keefe & Burgess, 1996) and with established computational models of place field generation  
253 by BVCs (Barry et al., 2006). This connectivity has been pre-trained dependent on the perceived layout of  
254 the room and the agent’s location. Hence the agent treats walls as stable, while smaller objects can move.  
255 The configuration of BVCs that is consistent with the given location has synaptic connections with a cluster  
256 of place cells for that given location (and vice versa for recall). For the purposes of the integrated model, the  
257 spatial memory component assumes that parts of the visual system can extract the distance and egocentric  
258 directional information of boundaries from retinal inputs. This is not explicitly modelled and relies on cues  
259 from the VR (Fig. 2, world information). A network that performs these computations could be learned (Lian  
260 et al., 2023), but this mechanism is beyond the scope of the present manuscript.

### 261 2.2.6. Model Specification

262 Spacecog is built on the foundation of several previously published models, and detailed information about  
263 the neural models and their underlying assumptions can be found in these works as outlined in the previous  
264 sections. As these models have already been fitted to experimental data, most of the parameters in visual  
265 and spatial areas remain unchanged. The present model focuses on more holistic aspects, which allows us to  
266 explore more complex and complete tasks through the integration of memory and vision through parietal

267 areas. This part of the model requires an interaction of visual and spatial neural populations, which operate  
268 in different coordinate systems. While head-centered information in both  $X_h$  and PWO is two-dimensional, the  
269 representation in PWO changes from a visual field (height and width) to a birds-eye spatial map (left/right,  
270 radial distance) as visible in Figure 6. Thus, while other populations in the model are fully connected on a  
271 neural level, this transition requires additional information. During bottom-up encoding processes, only the  
272 horizontal component of the  $X_h$  signal is used and supplemented with externally provided depth information  
273 from the VR before being used as an object cue for PWO. In return, this loses the height-dimension of the  
274 visual field, which is stored externally to be used during the back-transformation in the recall phase.

275 Further, a sensible balance between feature-based and spatial attentional mechanisms needs to be found.  
276 As feature-based attention originates in PFC and directly modulates V4/IT activities, the spatial attention  
277 pointer during recall originates in OVC and has to be looped back all the way into visual areas. For this,  
278 in addition to the already established recurrent V4/IT-FEF loop, we expanded the model by a recurrent  
279 V4/IT→LIP→FEF<sub>v</sub>→FEF<sub>vm</sub>→V4/IT loop, consistent with the idea that a connection between these areas  
280 could act as a simple representation of attentional priority, which is also fed back into visual areas (Bisley &  
281 Mirpour, 2019). Also the ventral stream model was adapted. Learning was conducted via the more simple  
282 and fast one-shot learning (Jamalian et al., 2016), rather than Hebb-type trace learning (Beuth, 2019). The  
283 pooling inside V1 and the pooling from V1→V4/IT was adapted, so the receptive fields of a V4/IT neuron  
284 are large enough to fit the relevant objects. Thus, some parameters in the mentioned areas were tuned by  
285 hand to facilitate such behaviour. As a result, the model is able to robustly encode objects into memory and  
286 to use this knowledge as spatial attentional information to enhance re-localisations of previously encoded  
287 objects. Further, we will also show that this structure of the model allows for the observation of perceptual  
288 neglect-like behaviour when a lesion is introduced in the parietal  $X_h$  priority map.

### 289 *2.2.7. Model Implementation*

290 The neurocomputational model is implemented with ANNarchy 4.7.1.1 (Vitay et al., 2015). ANNarchy  
291 (Artificial Neural Networks architect) is a neural simulator designed for distributed rate-coded or spiking neural  
292 networks. The user-interface is written in Python and uses an equation-oriented mathematical description  
293 of the neuron and synapse models. From this description, ANNarchy will generate efficient C++ code to  
294 perform the network simulation on parallel hardware.

295 We provide the complete source code for the model and the virtual environment, which is publicly accessible  
296 through [https://github.com/hamkerlab/Burkhardt2023\\_SpatialCognition](https://github.com/hamkerlab/Burkhardt2023_SpatialCognition). With the provided code, the  
297 simulations introduced in the present paper can be replicated and freely modified (limited to the pre-trained  
298 spatial environment of the room and the three target objects). Due to the large size of the model, a complete  
299 description of the network can be found in the supplementary material. This includes the equations for all  
300 neural populations as well as all parameters and connections used. More detailed information about the neural  
301 models and their underlying assumptions can also be found in the previously published works (Bicanski &

302 [Burgess \(2018\)](#); [Beuth \(2019\)](#); [Bergelt & Hamker \(2019\)](#)).

### 303 **3. Results**

304 To evaluate the performance of our model, the cognitive agent Felice has to perform tasks in the virtual  
305 environment, which were developed to emulate a real-life situation requiring features of spatial cognition such  
306 as object localisation, attentive dynamics, coordinate transformations, and spatial memory and imagery. We  
307 first introduce the general structure of an integrated task combining these requirements, and later evaluate it  
308 through multiple experiments, modifying individual parts of our model and tasks.

#### 309 *3.1. General Task*

310 Let us assume the following scenario: Felice first wants to play with one of her toys (e.g. a green toy crane),  
311 which she is able to localise among several other toys on her desk. She then gets distracted by another task  
312 and ends up at a different location in the room. From there, Felice decides she wants to again play with the  
313 toy crane, remembers where she initially found the toy and subsequently walks back to the location where she  
314 initially spotted the crane in order to localise it again. For this, we will use ego-, and allocentric information  
315 as outlined in the model description, but not relative information such as "on the desk". Decisions about  
316 'when to do what' are pre-defined, as decision making is not a particular focus of this study.

317 Generally, the task can be divided into an encoding phase and a recall phase. In the encoding phase, Felice  
318 has to find and encode an object into memory, which incorporates the entire process of using eye-centred visual  
319 information and transforming it into allocentric representation of objects and space in long-term memory.  
320 More specifically, starting from an arbitrary position, Felice walks into the vicinity of potential target objects.  
321 In this case, a random position within a circular area in front of her desk is assigned as a plausible position  
322 (Figure 5, middle). While Felice is able to move freely within the boundaries of her room, path planning and  
323 walking is not part of our model and was achieved through a simple A\* search algorithm. Once she arrives in  
324 front of the desk, Felice aims to select one target among other potentially relevant objects. For simplicity, we  
325 here demonstrate this ability with three objects: A green and a yellow toy crane, as well as a green race car.  
326 Finding the target among a combination of these objects covers the main challenges for the object localisation,  
327 namely a similarity in shape and/or colour for the distractor objects. Additionally, features of the room itself  
328 can also be regarded as distractors, as neurons might respond to edges or colour gradients in them. After  
329 Felice successfully localises the object, its position and identity as well as the position of Felice are stored in  
330 long-term memory in MTL (by learning connections between place cells and object vector cells).

331 Figure 6 displays the structure and activities of neuronal populations for the encoding phase. First, the  
332 visual field is pre-processed in V1, features are extracted in V4/IT, and spatial attention emerges from the  
333 recurrent V4/IT-FEF loop. In parallel, this information is passed to LIP, where a coordinate transformation  
334 takes place to transform the object position from a retinotopic into a head-centred reference frame in  $X_h$ . From  
335 there, object and spatial boundary information are formed in the parietal window and this (head-centred)

336 information is then transformed into an allocentric reference frame via RSC and encoded into long-term  
337 memory in MTL populations.

338 Felice then walks to a different position, from where the recall phase shown in Figure 7 is triggered. **The**  
339 **recall phase consists of Felice remembering, walking back to, and re-localising a previously encoded object.**  
340 **This process starts by applying an externally provided cue to the P<sub>Ro</sub> neuron coding for the previously**  
341 **encoded object ("I want my green crane!"), which can be understood as an "eyes-closed remembering", with**  
342 **no interference from the current perceptual input.** The resulting memory recall re-establishes information  
343 about the position of Felice and the memorised object from the time of encoding in the MTL attractor  
344 network. Specifically, Felice is then able to decode her previous position and body orientation from PC and  
345 HD activities and walks back to this recalled position. **For this purpose, we read out PC and HD firing rates**  
346 **after memory recall and use this for external navigation. Once she arrives at the desk, Felice again searches**  
347 **for her green crane. The re-localisation of the target object can take place in three different ways: In the**  
348 **first way, Felice can use feature-based attention from PFC (as in the encoding phase shown in Figure 6) to**  
349 **re-localise the object. This can intuitively be construed as Felice remembering that she has previously seen**  
350 **the desired object from a particular position (e.g. close to the table), but she has no access to its exact**  
351 **location. In the second way, Felice uses recalled spatial memory information that is looped back through the**  
352 **PW (Figure 7) and being used for a spatial attention pointer generated in  $X_h$ . The spatial attention pointer**  
353 **biases the neural dynamics within the visual system to guide visual search (without feature-based attention),**  
354 **corresponding to Felice recalling where the target object is located, without remembering its exact identity.**  
355 **Third, a combination of both options (feature-based attention combined with a spatial attention pointer) can**  
356 **be used, meaning Felice now recalls the location and relative direction as well as the identity of a previously**  
357 **encoded object.**

358 To test these conditions, we introduce two different experimental settings (normal and cluttered scene),  
359 which cover the integration of vision and memory in slightly different scenarios. As the model operates in a  
360 realistic setting, we assess its behavioural performance through successful trial completions and the duration  
361 needed for each object localisation. The main purpose of the evaluation is to demonstrate the spatio-cognitive  
362 ability by means of a brain-inspired model. Further, we report and discuss differences observed in the sketched  
363 ways to perform the task.

### 364 *3.2. Experiment 1: Spatial memory and object recognition in a normal scene*

365 Experiment 1 is performed in an environment containing three potential target objects (Figure 8). The  
366 three possibilities of using attentional mechanisms for object localisation in the recall phase described above  
367 are used to assess the integration between vision and spatial memory.

#### 368 *3.2.1. Experiment 1.1: Spatial memory and object recognition using feature-based attention*

369 Initially, Felice was asked to walk into the vicinity of potential target objects, where the first object  
370 localisation was performed randomly for one of the three objects. Thus, our model is run by setting an

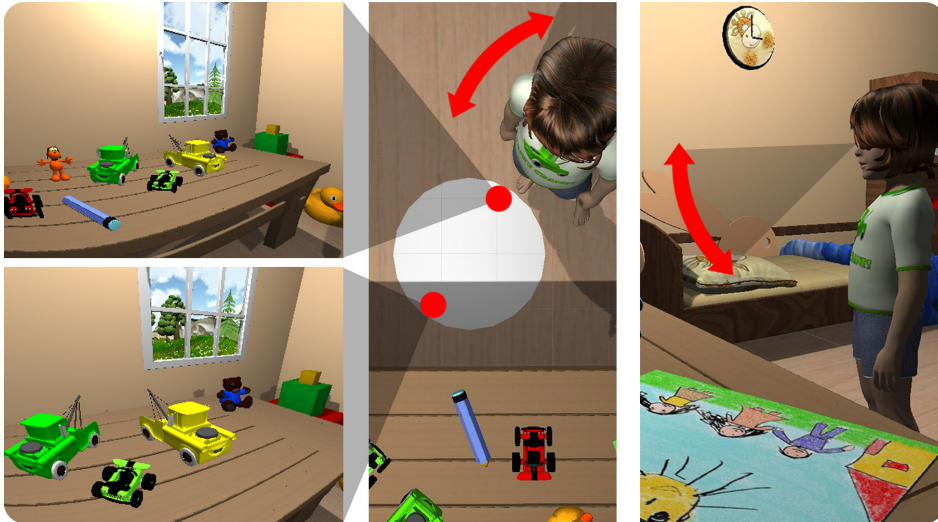


Figure 5: General scenario. The cognitive agent Felice performs a combined task of memory encoding and recall. Illustrated here is the encoding phase, in which Felice walks into the vicinity of target objects (random position within the white circle shown in the middle image). Depending on her position, body orientation and head tilt are adjusted to ensure the visibility of all potential target objects (middle, right). Variability in this adjustment results in different random views of the scene (left). **The limiting factor for the positional variability is the spatial resolution of the visual layers V4/IT, and therefore the size of the objects in the visual field, which was controlled for by the allowed positions for object localisation (white circle).**

371 activation for the target object in PFC, which allows feature-based attention to support target localisation.  
 372 Then, after shifting gaze to the target object, the integrated model encodes the object and positional  
 373 information into long-term memory. This corresponds to the encoding phase displayed in Figure 6 and was  
 374 performed for total of 100 times. In each trial, a random target object and a random agent position (within  
 375 the white circle displayed in Figure 5) were chosen, which resulted in a successful object localisation in 93% of  
 376 trials (Table 1, first row).

377 In each trial, Felice then walked to a different position in the room, from which the encoded object was  
 378 not visible and recalled her memory by activating the P<sub>RO</sub> cell of the previously encoded object. Part of  
 379 this memory is her previous position (encoded by place cells) and the corresponding object location in the  
 380 room (Figure 7). Felice then walked to the recalled position and performed a re-localisation of the previously  
 381 encoded object. In this experiment, she used feature-based attention from PFC, and subsequently performed  
 382 a saccade to the selected candidate object. If the object was correctly re-localised, the trial was labelled as  
 383 successful. We therefore define a successful recall as a correct completion of the complete task, which includes  
 384 the encoding and recall phase. This resulted in a success rate of 95% (Table 1, second row), which marginally  
 385 differs from the encoding phase due to small deviations in Felice’s position during recall.

386 We found the success in this experiment to be mainly dependent on two factors: First, the visual part  
 387 of the model performing a correct object localisation and second, the spatial part of the model accurately  
 388 encoding the positional information, enabling Felice to precisely return to the location of the previously



389 encoded target object. However, as the second object localisation in this experiment also only required  
 390 feature-based attention, the positional memory was not required to be extremely accurate. All errors in this  
 391 experiment therefore were a result of the visual part of the model incorrectly localising the object. We will  
 392 consider this result as a baseline and compare it to results from Experiment 1.2 and 1.3.

Table 1: Performance of the model (N=100).

| Task     | Experiment  | Attention               | Success rate | Simulation steps (M $\pm$ SD) |
|----------|-------------|-------------------------|--------------|-------------------------------|
| Encoding | 1.1,1.2,1.3 | Feature-based           | 93%          | 150 $\pm$ 57                  |
| Recall   | 1.1         | Feature-based           | 95%          | 154 $\pm$ 59                  |
| Recall   | 1.2         | Spatial                 | 83%          | 172 $\pm$ 48                  |
| Recall   | 1.3         | Spatial + feature-based | 94%          | 125 $\pm$ 10                  |

393 *3.2.2. Experiment 1.2: Spatial memory and object recognition using a spatial attention pointer from memory*

394 In the second experiment, rather than feature-based attention, a spatial attention pointer from the memory  
 395 recall via LIP was used to perform the second object localisation after Felice returned to the previously  
 396 encoded target object. During recall, allocentric information of the object position are transformed through  
 397 RSC into head-centred activity in the parietal window. After Felice returns to the place where she encoded the  
 398 target object, this information is subsequently used in  $X_h$  and LIP to generate a retinocentric spatial attention  
 399 pointer. An advantage of using spatial attention provided by LIP is that it does not require extensive visual  
 400 search to localise the target object.

401 We observed that without the aid of feature-based attention, the spatial attention pointer from long-term  
 402 memory alone could generate a success rate of 83% (Table 1). Compared to Experiment 1.1, this is a slight  
 403 decrease in performance, which was mostly caused by two factors: First, even small inaccuracies in the  
 404 positional recall of Felice (decoded from PCs) were able to change the resulting visual field to a degree in  
 405 which the spatial attention pointer was slightly misplaced. Second, inaccuracies in the recalled position due to  
 406 a limited spatial resolution of neural populations (each PWO and OVC cell covers a  $7^\circ$  bin of the visual field)  
 407 could also lead to a small, erroneous shift of the attention pointer, even though a weighted average approach  
 408 was used to decode this information. Despite these limitations, only a few additional errors occurred, mostly  
 409 in cases in which two objects were close to each other (Figure 8, Experiment 1.2).

410 *3.2.3. Experiment 1.3: Spatial memory and object recognition using a combination of feature-based attention  
 411 and a spatial attention pointer from memory*

412 Experiment 3 combined both information sources about the object, namely spatial and feature-based  
 413 attention, in the recall phase. This increased the performance back to the level of encoding and therefore  
 414 mitigated errors previously introduced by spatial attention (Figure 8, Experiment 1.3). Additionally, as

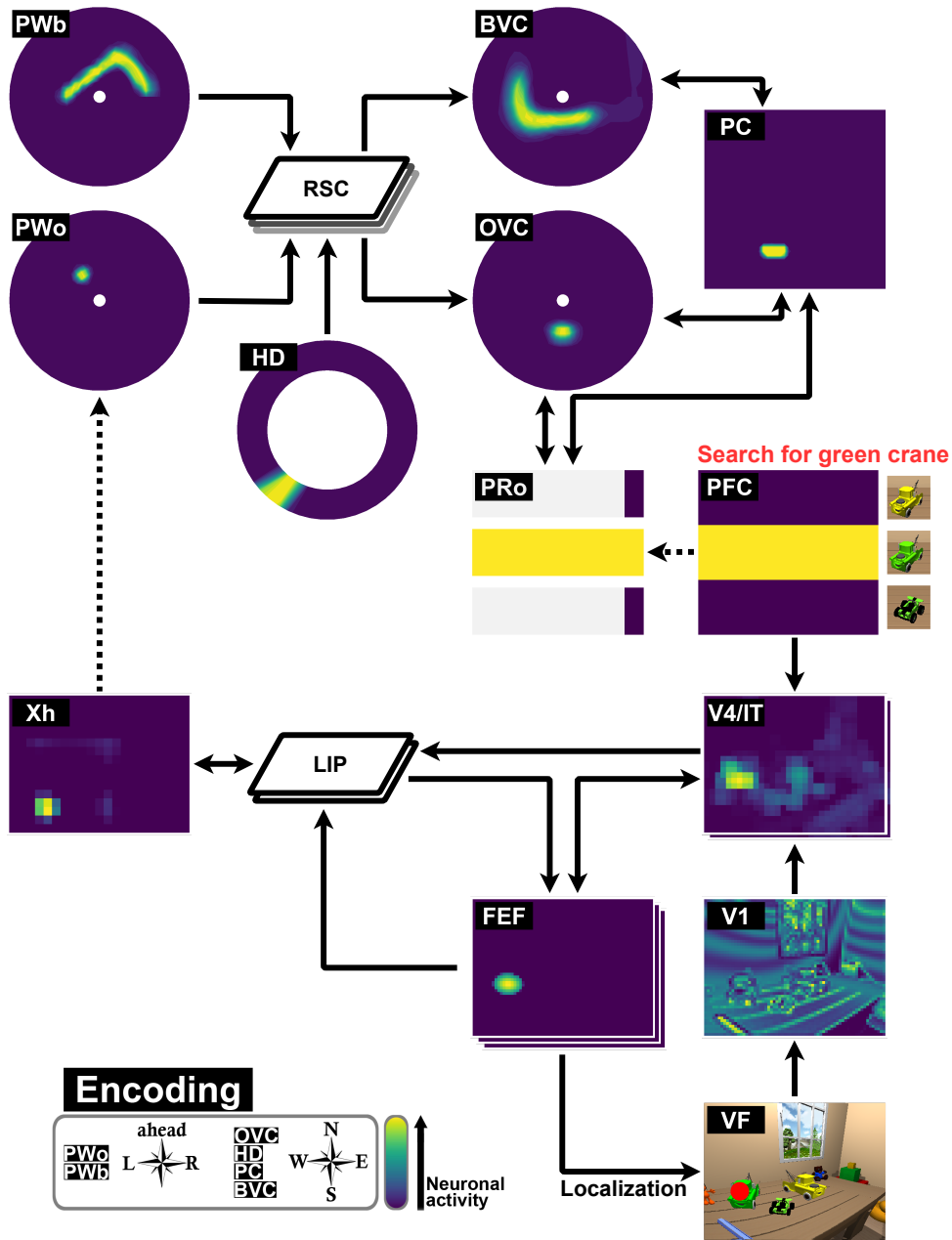


Figure 6: A representative subset of neural activity for the encoding phase of the general task of visual search and object memory (not included: V4/IT L4, FEFv, FEFvm, PRb). For encoding, the visual field (VF) is processed by V1 neurons and fed into higher visual areas. There, object neurons in V4/IT L2/3 are guided by feature-based attention from PFC and spatial attention emerges via FEFvm feedback to V4/IT until FEFm triggers a saccade towards the object. Spatial information is transformed from a retinocentric into a head centred reference frame in area LIP and gives rise to activity in X<sub>h</sub>, where it is used as a head-centred input for parietal window object neurons (PWO) encoding the spatial position of the object relative to the agent (here ahead-left). This requires externally provided depth information from the virtual environment, while height information has to be saved for the recall phase. Combined with information of the boundaries of the room (PWb) as well as head direction (HD), this information is transformed through RSC, resulting in allocentric representations of the object location (OVC), boundaries (BVC), and agent position (PC) being established in MTL, where they are encoded into long-term memory.

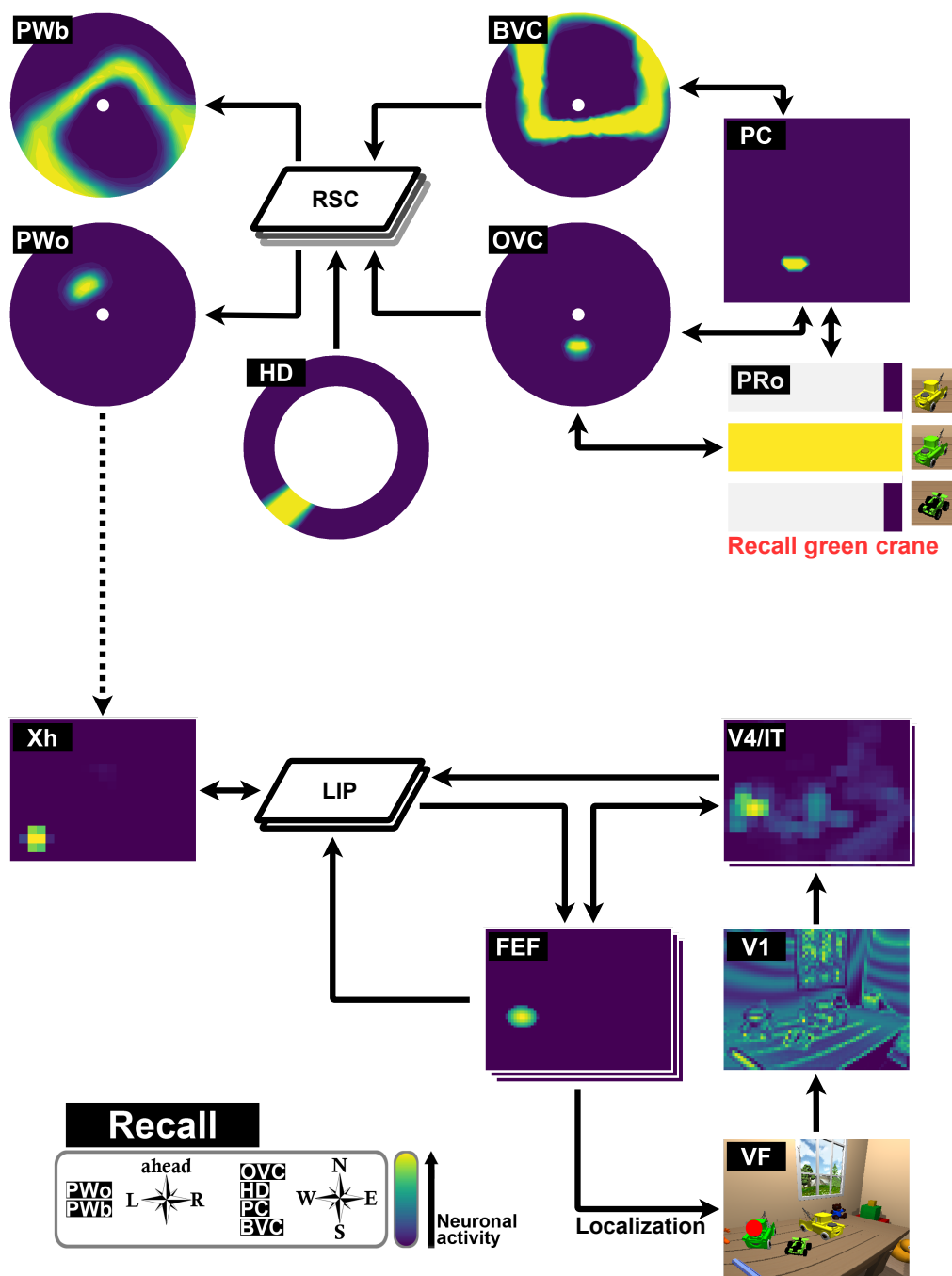


Figure 7: A representative subset of neural activity for the recall phase of the general task of visual search and object memory (not included: V4/IT L4, FEFv, FEFvm, PRb). From a remote position in the room, a recall of the previously encoded object is triggered through PRo activation. This re-establishes activity in the MTL attractor network (OVC, BVC, PC) as well as in HD populations. Through RSC, this information is transformed into a head-centred reference frame in PWO and PWb. Information of the object position can then be fed back into Xh, from which a retinocentric spatial attention pointer can be established in area LIP. With this top-down attention signal being applied on FEFv, the position of the object can then be decoded from the build-up movement neurons in FEFm. Once an activity threshold in FEFm is reached, a saccade is performed towards the target object.

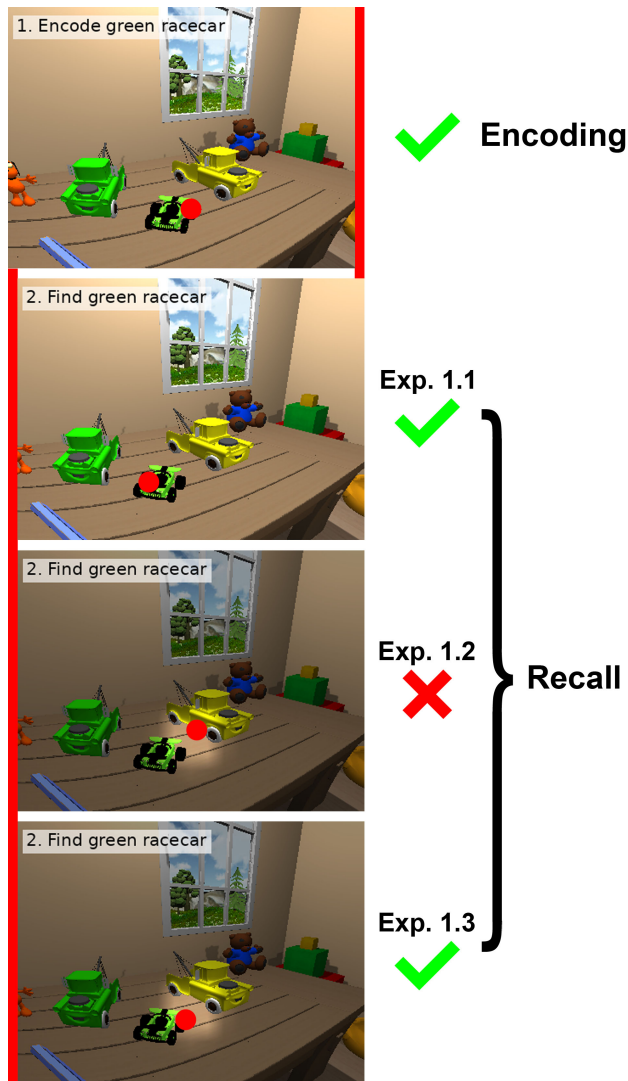


Figure 8: Experiment 1. Felice initially encodes the green race car. Small inaccuracies in the spatial memory can lead to a slightly different agent position during recall and therefore also a slight shift in the visual field (the red bars display the alteration in the visual field between encoding and recall phase, which result in a shift to the right). Results from the recall phase of all three experiments are shown (Experiment 1.1 uses only feature-based attention, Experiment 1.2 uses only a spatial attention pointer, and Experiment 1.3 utilises both feature-based and spatial attention). Shifts in the visual field do not affect feature-based attention used in Experiment 1.1, but can lead to ambiguous situations in Experiment 1.2, in which the spatial attention pointer is placed between two objects. If the spatial attention pointer is however combined with feature-based attention (Experiment 1.3), these ambiguities can be resolved.

415 the spatial attention pointer was quickly available to assist during feature search, the time required for a  
 416 successful re-localisation was reduced by 27% (Table 1). Therefore, the spatial attention pointer was able  
 417 to guide the object localisation effectively, while feature-based attention compensated potential ambiguities  
 418 through inaccuracies introduced through memory and imagery processes.

#### 419 *3.2.4. Neural dynamics for target selection*

420 As the observed time for target selection varies in Experiments 1.1, 1.2, and 1.3 (Table 1), with the  
421 combination of feature-based and spatial attention being fastest, we analysed the temporal dynamics in the  
422 model (Figure 9). Feature-based attention operates across the entire visual scene and increases the gain  
423 of those neural responses where visual input and target template matches. Thus, neural activity in V4/IT  
424 is enhanced at the target location. Spatial attention recalled from memory traverses via  $X_h$  and LIP into  
425 the visual system and increases the activation at the target location if the recall from memory is correct.  
426 Recurrent dynamics lead to an exchange of activity across the whole visual parts, but they converge in FEF  
427 which enforces saccade target selection from FEFv, FEFvm to FEFm cells. If feature-based attention is  
428 used (Experiment 1.1 and 1.3), V4/IT has a higher activity than in Experiment 1.2, where only a spatial  
429 attention pointer is used for the localisation of the target object. In contrast, a spatial attention pointer leads  
430 to higher input from LIP in Experiment 1.2 and 1.3. Together, this results in the fastest rise of activity in  
431 FEFv for Experiment 1.3 and therefore the earliest initialisation of a saccade through FEFm among all three  
432 experiments.

#### 433 *3.3. Experiment 2: Spatial memory and object recognition in a cluttered scene*

434 The previous experiments were all performed in the same general scene setting, where only the three target  
435 objects were presented in both encoding and recall phase as shown in Figure 8. Experiment 2 changes this  
436 by cluttering the scene between the memory encoding and the recall phase by placing additional toys onto  
437 the desk hiding the targets (Figure 10). This results in a much more challenging scenario and thus allows us  
438 to gain further insight into the interaction of memory and vision. Again, we distinguish between the three  
439 possibilities using attentional mechanisms for the object localisation in the recall phase. The summary of the  
440 results for this experiment is shown in Table 2.

##### 441 *3.3.1. Experiment 2.1: Feature-based attention*

442 As the encoding phase is identical to previous experiments, we again observe a success rate of 93%.  
443 However, in the recall phase the object localisation now has to be performed in the cluttered scene, which  
444 dropped the performance to 27%, while the time required for a successful localisation increased to 231 steps,  
445 combined with a significant higher standard deviation, when only feature-based attention was used. As no  
446 spatial memory was used to aid the object localisation, the reduction in performance can solely be attributed  
447 to the visual model being unable to rely on enough features of the target objects, which are now substantially  
448 covered by other objects.

##### 449 *3.3.2. Experiment 2.2: Spatial attention from memory*

450 In comparison to Experiment 1.2, this study uses only a spatial attention pointer from memory to perform  
451 the object localisation in the recall phase. This results in a further drop in performance to 14% and an  
452 increased localisation time of 239 steps. In addition to features of the target objects being covered by the

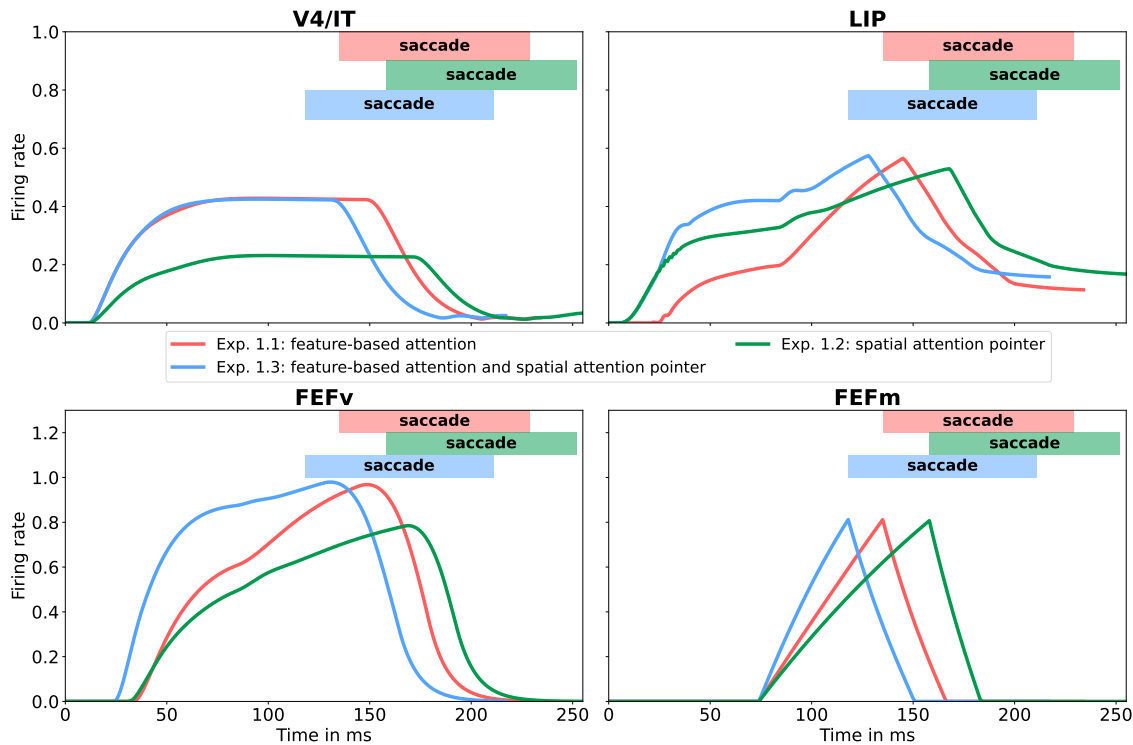


Figure 9: Analysis of temporal dynamics that lead to different reaction times across experiments. Plotted traces reflect the activation at the target location in different parts of the model. In conditions where visual search recruits feature-based attention, V4/IT activity increases due to the match of the visual input with the target template. In conditions where a spatial attention pointer from memory is recalled, the activation of LIP cells at the target location is increased. As FEFv cells collect information from those different parts of the model and pass it to FEFm to enforce a final decision about the saccade target, they reflect both biases in their activation. A saccade can be initialised fastest, if both feature-based attention and a spatial attention pointer are used. Shown are feature independent, pooled firing rates of V4/IT, Layer 2/3 (top left), and firing rates of LIP (top right) representing the target location, which both serve as input to FEFv (bottom left), as well as the firing rates of FEFm (bottom right), which trigger the saccade. Activation of a typical trial in each of the three Experiments 1.1 (red), 1.2 (green), 1.3 (blue) are plotted over time. The period of the saccade is marked for each experiment.

453 distractor objects, small inaccuracies in the position of the spatial attention pointer further contribute to  
 454 the reduction in performance like in Experiment 1.2. It is to note that, while previous unsuccessful trials of  
 455 object localisation almost always meant the selection of an incorrect object, in this experiment 84% of errors  
 456 result from a timeout (FEFm activity not reaching a saccade threshold after 600 simulation steps). This is a  
 457 direct limitation introduced by the small codebook of the visual model, which only includes three pre-trained  
 458 objects, and therefore has no knowledge about the identity of the additional distractor objects. As V4/IT  
 459 feeds the FEF, not much activity is transmitted across this pathway, which leads to an overall lesser activity  
 460 in the visual system including FEFm. An additional putative method of compensation would be stronger  
 461 self-excitation parameters in the saccade system to enforce saccade targets even into weakly activated areas.  
 462 However, we kept all parameters unchanged to directly compare the different experiments.

463 *3.3.3. Experiment 2.3: Combination of feature-based and spatial attention from memory*

464 This simulation combines the attentional mechanisms of feature-based attention and the spatial attention  
 465 pointer from memory during recall in a cluttered scene. The performance in this simulation increases to 48%  
 466 while the average time required for a successful object localisation is reduced to 194 simulation steps. The  
 467 main novelty of this simulation can be seen in comparison to Experiment 1, where the combination of both  
 468 attentional mechanisms in Experiment 1.3 only recovered the reduction in performance back to the baseline  
 469 level. This increase in performance for Experiment 2.3 further underscores the advantages of integrating  
 470 spatial memory with vision, especially in challenging environments.

Table 2: Performance in cluttered scenes (N=100).

| Task     | Experiment  | Attention               | Success rate | Simulation steps (M $\pm$ SD) |
|----------|-------------|-------------------------|--------------|-------------------------------|
| Encoding | 2.1,2.2,2.3 | Feature-based           | 93%          | 150 $\pm$ 57                  |
| Recall   | 2.1         | Feature-based           | 28%          | 231 $\pm$ 73                  |
| Recall   | 2.2         | Spatial                 | 14%          | 239 $\pm$ 99                  |
| Recall   | 2.3         | Spatial + feature-based | 48%          | 194 $\pm$ 69                  |

471 *3.4. Experiment 3: Visual Neglect*

472 This simulation aims to further highlight the biological plausibility of our model by demonstrating that a  
 473 simple impairment in a parietal area leads to similar behaviour as observed in patients with visual neglect.

474 Visual neglect is one of the most notable impairments resulting from damage to parietal areas of the brain,  
 475 and is known to cause impairments in directional processes of attention and localisation of objects, resulting  
 476 in a lack of responses to stimuli in parts of the visual field (Bartolomeo, 2007). This is thought to correspond  
 477 to damage in a parietal priority map, which integrates goal and stimulus related signals for spatial selection  
 478 (Bays et al., 2010). In our model, we can observe similar effects by introducing an impairment to  $X_h$  neurons  
 479 corresponding to the left half of the visual field. This is implemented by removing all connections between  
 480 LIP and the left half of  $X_h$  neurons, generating visual perceptual neglect.

481 Figure 11 depicts a simulation with two identical objects. Since feature-based attention favours both  
 482 objects, the model converges on one of the cranes, depending on the exact spatial arrangement (position of  
 483 agent and objects). In the depicted scenario, the left crane is chosen as the preferred stimulus, which is mostly  
 484 visible in FEFm and  $X_h$  population activity (Figure 11, top). Consequently, a saccade is made to the left  
 485 crane (visualised by the red dot in Figure 11, top right)

486 Introducing left visual neglect in an identical simulation results in only the right crane being active in  
 487 the  $X_h$  priority map, which then leads to a reduced response of the left crane in LIP. Subsequently, through  
 488 the recurrent LIP-FEF loop, this also creates a bias in FEF (Figure 11, bottom). There, bottom-up visual

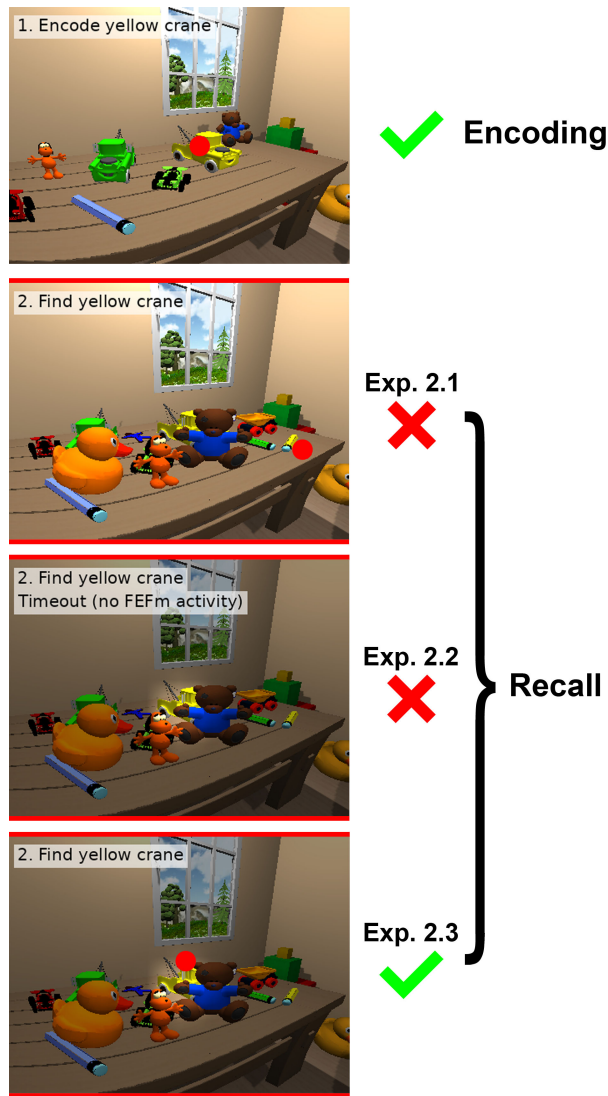


Figure 10: Experiment 2. In this condition, the scene is cluttered in the recall phase with additional distractor objects which cover the original target objects to a large degree. This creates a highly challenging task. In Experiment 2.1, the model is not able to re-localise the yellow crane, as most of its features are hidden behind the teddy bear. Experiment 2.2 with only spatial attention also fails despite a correct spatial attention pointer as no FEFm activity is formed due to a lack of V4/IT activity. Only in experiment 2.3 a successful re-localisation of the yellow crane is performed due to the combined application of feature-based and spatial attention. The red bars indicate the alteration in the visual field during recall, which in this case is the result of Felice recalling a position slightly closer to the table compared to the encoding phase. Here, this deviation is negligible and does not result in a misplacement of the spatial attention pointer.

489 input is modulated by attentional input from LIP, which leads to a saccade directed to the crane on the right  
 490 (red dot in Figure 11, bottom right). Thus, although object recognition and initial spatial attention via FEF  
 491 are unaffected by the impairment, a bias emerges in the additional recurrent LIP-FEF loop, which results in  
 492 behaviour similar to visual neglect. Additionally, as  $X_h$  forms a bridge between visual and spatial areas, only  
 493 the position of the right object will be passed to the parietal window and is encoded into memory. Visual



494 neglect is therefore also present in memory and imagery.

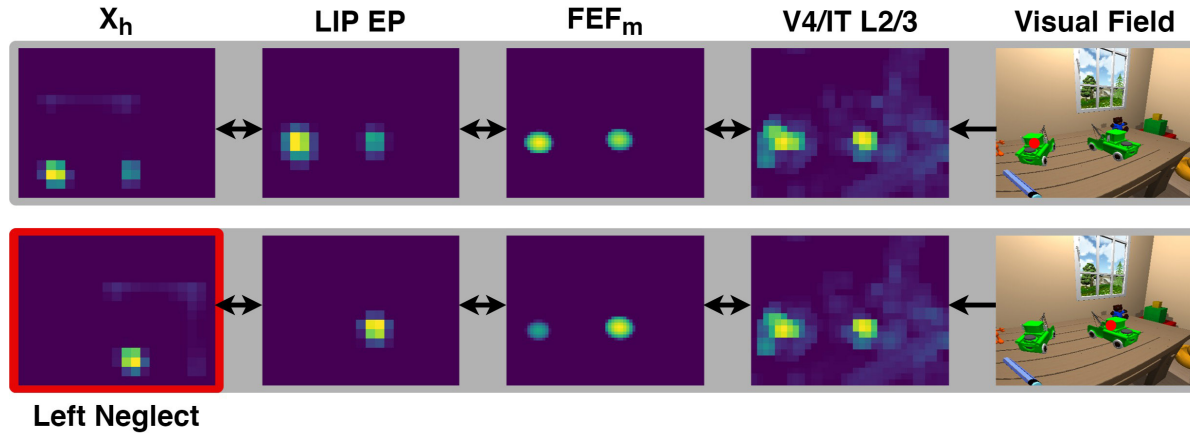


Figure 11: Visual neglect. In the top row, a typical simulation is shown, which results in the left crane being selected for a potential saccade ( $F_{EFm}$ ). When left side visual neglect is introduced in  $X_h$ , activities for the right object are projected back into FEF via LIP, while reentrant processing between LIP and FEF is weakened in the left visual field (bottom row), and as a result, the right object is selected as the saccade target.

#### 495 4. Discussion

496 We have introduced the Spacecog model, a biologically motivated, large-scale neurocomputational model  
497 of spatial cognition, which we tested and evaluated in a real-world-like virtual environment. Via a coherent  
498 processing stream incorporating perceptual vision processes, attentive dynamics, and spatial memory and  
499 imagery, Spacecog is able to display key traits of spatial cognition. The underlying individual models  
500 were previously verified on their own and are motivated and grounded by anatomical, behavioural, and  
501 physiological data. While aspects specific to these individual components have already been described in  
502 previous publications, we here focused on the integration and interplay between memory and vision through  
503 parietal areas.

504 In three experiments, interactions between visual and spatial areas were evaluated and it was shown  
505 how the integration enables the agent to successfully perform tasks of object localisation and imagery.  
506 In all experiments, the agent was able to robustly detect and memorise objects. The introduction of a  
507 spatial attention pointer from memory by itself was able to generate a high success-rate during recall, but  
508 also introduced an increase in the time required for localisation due to the interplay of model components  
509 (Experiment 1.2). An integrated use of spatial and feature-based attention combined the advantages of a quick  
510 availability of the spatial attention signal from memory with the accuracy of feature-based attention to allow  
511 for a faster and robust re-localisation of objects (Experiment 1.3). **Additional advantages of integrating spatial  
512 memory with vision were further explored in a cluttered environment, which showed that this integration is  
513 crucial for an adequate performance in even more challenging tasks (Experiment 2).**

514 Notably, in conditions with only feature-based attention (Experiment 1.1/2.1), the agent was already  
515 successful in localising the target object. It therefore is important to clarify that the conditions for search with  
516 only feature-based attention were chosen to be optimal, as it was ensured that the agent was in close proximity  
517 to the objects, and the target object was ensured to be in her field of view. Without this, under normal  
518 conditions, a more extensive visual search including overt orienting responses would have been necessary. This  
519 also implies that during phases of recall, the recalled position and head direction are always used to guide the  
520 agent back to the target object, even when no direct interface between memory and vision through PW and  
521 LIP was established (Experiment 1.1/2.1). The good performance in only feature-based attention was also  
522 based on the fact that we did not use heavily cluttered scenes, and feature-based attention was still effective  
523 in guiding attention to the target. If we were to use more difficult search scenes, the search process would  
524 require multiple saccades, and thus the benefit of spatial memory would be more obvious. In such cases, the  
525 model would require an additional circuit to implement inhibition of return (Hamker, 2005a).

526 However, the main novelty is not the use of spatial or feature-based signals for object recognition, but the  
527 ability to establish spatial and object memory and to use this memory to guide vision. If agents are able  
528 to recall and use information about spatial proximity, gaze direction, feature-based attention, and spatial  
529 attention, they can accurately and efficiently re-localise previously encoded objects. This is a combination  
530 which has not yet been demonstrated in previous biologically motivated models. We underlined the robustness  
531 of this ability by allowing variability in the encoding process, resulting in different views of the scene.  
532 Furthermore, consistent with the idea that neglect results from damage in a parietal priority map (Bays et al.,  
533 2010), it was also shown that parietal lesions in our model can produce neglect-like behaviour (Experiment  
534 3). **Our integrated model therefore extends the mechanisms by which previous models accounted for spatial  
535 representational neglect (Byrne et al., 2007; Bicanski & Burgess, 2018) to neglect in the visual field.**

536 The present model underlines the importance of the parietal cortex as an interface between vision and  
537 memory. Early concepts of the parietal cortex have already emphasised its role in providing 'where' information  
538 about the object (Mishkin et al., 1983), but were later extended with respect to actions towards objects  
539 (Milner & Goodale, 1995) and visual attention (Colby & Goldberg, 1999; Gottlieb, 2007), and more recently  
540 also with its role in episodic memory retrieval (Becker & Burgess, 2000; Cabeza et al., 2008; Sestieri et al.,  
541 2017; Connor & Knierim, 2017).

542 **Further, the present model can be compared with experiments on human spatial cognition that show that  
543 long term spatial memory interacts with visual attention behaviourally, and reflects parieto-prefrontal activity  
544 related to attention and hippocampal and parahippocampal activity related to the benefit from long term  
545 memory (Summerfield et al., 2006). Our model can address the behavioural advantage for memory-cued  
546 locations (Experiment 1.3 and 2.3) and also its relation to the activity in different regions. A prediction from  
547 our model might be that hippocampal and retrosplenial activity correlate with performance more strongly  
548 when the target was previously seen in location from a different viewpoint, so that purely visual memories  
549 cannot give an advantage. Additionally, behavioural hypotheses could further be tested in identical virtual**

550 environments, as gaze behaviour in the context of locomotion was recently shown to be highly similar in  
551 virtual environments and the real world (Drewes et al., 2021).

552 Even though the complexity of the parietal and temporal cortex is much beyond what we cover with our  
553 model, our account proposes a framework of how memory recall can directly guide visual perception by means  
554 of transformation from allocentric to egocentric reference frames and visual attention. Thus, our Spacecog  
555 model demonstrates for the first time an integrated account of memory and vision.

556 Despite the model already covering some aspects of spatial cognition, it is by no means complete. Felice  
557 only uses monocular vision and we do not extract any depth information from the image by stereo vision  
558 or optic flow. Thus, despite her ability to recall and visit her recalled position in space, her understanding  
559 of space is limited due to missing depth information. Hence, in the present model, boundary information  
560 (the walls of the room) is supplemented by the VR and not the result of visual perception. The Spacecog  
561 model on which she operates also does have only a limited form of scene memory, while humans can store a  
562 large number of scene representations in visual long-term memory (Konkle et al., 2010), which may support  
563 self-localisation and allow to locate objects as part of the scene context (Hollingworth, 2007).

564 A further limiting factor of the model is computational complexity, which is most visible in the interaction  
565 of spatial and visual areas. Due to limits in the spatial accuracy of neural populations, small inaccuracies  
566 can occur during encoding and recall, which can lead to shifts in the position of the agent and its visual  
567 field, or in the placement of spatial attention. Increasing neural populations to more realistic numbers would  
568 be an obvious solution in this regard, however a performance-accuracy trade-off has to be made. Further,  
569 the development of biologically plausible but still efficient methods of object recognition is still an active  
570 research domain (Teichmann et al., 2021), while machine learning methods that rely on supervised learning  
571 are presently more powerful.

572 With respect to attention, it has been shown that the best possible search template are not necessarily the  
573 features of the to be searched object, but those features which best discriminate the target from distractor  
574 objects (Navalpakkam & Itti, 2007; Maith et al., 2021). Our present version of this model does not make use  
575 of learning a suitable top-down feature-based attention signal, given the context of a scene.

576 Finally, an important area of present and future research is the general flexibility of the agent. As outlined  
577 in the general task, the structure of the task is fairly fixed and Felice by herself is not given the ability to  
578 decide about her goals, plans and the outcomes of her actions. Thus, our model does not include reinforcement  
579 learning or other means of action selection. Although Felice is performing well in the specified task, this  
580 relies mostly on externally provided cues of where to initially walk and which object to attend to. Desired  
581 objects in encoding and recall are externally cued in the corresponding neural population and no intrinsic  
582 goal-directed behaviour is shown, as the required cognitive structures are not currently part of the model.

#### 583 4.1. Conclusion

584 The combination of visual, attentional and spatial components successfully bridges a gap between previously  
585 disparate areas of neurocomputational modelling. By introducing parietal areas as an interface between  
586 spatial and visual areas, this most notably creates the novelty of memory guided visual attention, which at  
587 this level has so far only been addressed by the presented model. In addition to the questions explored above,  
588 spatial information of previously encoded objects can now be used to explore attentional processes across eye  
589 movements. This can open up many new avenues concerning the interpretation of neuropsychological data  
590 in complex tasks of spatial memory and attention. The integrated model therefore also provides a unified  
591 framework for visuospatial tasks and can further be used as a powerful tool for the assessment of a broad  
592 spectrum of biologically rooted hypotheses concerning human spatial cognition.

#### 593 5. Data Availability

594 Code and data are available under [https://github.com/hamkerlab/Burkhardt2023\\_SpatialCognition](https://github.com/hamkerlab/Burkhardt2023_SpatialCognition).  
595 Due to the size of the network, we will provide the model description as an ANNarchy report in the  
596 supplementary information.

#### 597 6. Declaration of Interest

598 The authors declare no competing interests.

#### 599 7. Acknowledgements

600 A first version of this model has been funded by the European Union’s Seventh Framework Programme,  
601 grant number FP7-ICT 600785 Spatial Cognition. Funding by the German Research Foundation (DFG,  
602 416228727) - SFB 1410 Hybrid Societies and by the Saxony State Ministry of Science and Art (SMWK3-  
603 7304/35/3-2021/4819) research initiative ”Instant Teaming between Humans and Production Systems” on the  
604 basis of the budget passed by the deputies of the Saxony parliament, allowed us to further develop and verify  
605 the model. Additional funding was granted to Neil Burgess by the ERC advanced grant NEUROMEM.

#### 606 8. Author Contributions

607 **Micha Burkhardt:** Conceptualisation, Methodology, Software, Validation, Formal Analysis, Data Cura-  
608 tion, Writing - Original Draft, Writing - Review & Editing, Visualisation. **Julia Bergelt:** Conceptualisation,  
609 Methodology, Software, Validation, Writing - Review & Editing. **Lorenz Gönner:** Conceptualisation,  
610 Methodology, Software, Validation, Writing - Review & Editing. **Helge Ülo Dinkelbach:** Conceptualisation,  
611 Methodology, Software, Validation, Writing - Review & Editing. **Frederik Beuth:** Conceptualisation,  
612 Methodology, Validation, Writing - Review & Editing. **Alex Schwarz:** Methodology, Software, Validation.

613 **Andrej Bicanski:** Conceptualisation, Methodology, Writing - Review & Editing. **Neil Burgess:** Writing  
614 - Review & Editing, Resources, Supervision, Funding acquisition. **Fred H. Hamker:** Conceptualisation,  
615 Writing - Original Draft, Writing - Review & Editing, Resources, Supervision, Project administration, Funding  
616 acquisition

## 617 **References**

- 618 Antonelli, M., Gibaldi, A., Beuth, F., Duran, A. J., Canessa, A., Chessa, M., Solari, F., Del Pobil, A.  
619 P., Hamker, F. H., Chinellato, E., & Sabatini, S. P. (2014). A hierarchical system for a distributed  
620 representation of the peripersonal space of a humanoid robot. *IEEE Transactions on Autonomous Mental*  
621 *Development*, 6(4), 259-273. doi: <https://doi.org/10.1109/TAMD.2014.2332875>
- 622 Avraamides, M. N., & Kelly, J. W. (2008). Multiple systems of spatial memory and action. *Cognitive*  
623 *Processing*, 9(2), 93-106. doi: <https://doi.org/10.1007/s10339-007-0188-5>
- 624 Ballard, D. H., Hayhoe, M. M., Pook, P. K., & Rao, R. P. N. (1997). Deictic codes for the embodiment of cog-  
625 nition. *Behavioral and Brain Sciences*, 20(4), 723-742. doi: <https://doi.org/10.1017/S0140525X97001611>
- 626 Barry, C., Lever, C., Hayman, R., Hartley, T., Burton, S., O'Keefe, J., Jeffery, K., & Burgess, N. (2006). The  
627 boundary vector cell model of place cell firing and spatial memory. *Reviews in the Neurosciences*, 17(1-2),  
628 71-98. doi: <https://doi.org/REVNEURO.2006.17.1-2.71>
- 629 Bartolomeo, P. (2007). Visual neglect. *Current Opinion in Neurology*, 20(4), 381-386. doi: <https://doi.org/10.1097/WCO.0b013e32816aa3a3>
- 631 Bays, P. M., Singh-Curry, V., Gorgoraptis, N., Driver, J., & Husain, M. (2010). Integration of Goal- and  
632 Stimulus-Related Visual Signals Revealed by Damage to Human Parietal Cortex. *Journal of Neuroscience*,  
633 30(17), 5968-5978. doi: <https://doi.org/10.1523/JNEUROSCI.0997-10.2010>
- 634 Becker, S., & Burgess, N. (2000). Modelling spatial recall, mental imagery and neglect. In T. Leen,  
635 T. Dietterich, & V. Tresp (Eds.), *Advances in neural information processing systems* (Vol. 13). MIT Press.
- 636 Bergelt, J., & Hamker, F. H. (2016). Suppression of displacement detection in the presence and absence  
637 of eye movements: A neuro-computational perspective. *Biological Cybernetics*, 110(1), 81-89. doi:  
638 <https://doi.org/10.1007/s00422-015-0677-z>
- 639 Bergelt, J., & Hamker, F. H. (2019). Spatial updating of attention across eye movements: A neurocomputational  
640 approach. *Journal of Vision*, 19(7). doi: <https://doi.org/10.1167/19.7.10>
- 641 Beuth, F. (2019). *Visual attention in primates and for machines - neuronal mechanisms* (Doctoral  
642 dissertation, Department of Computer Science. Technische Universität Chemnitz). Retrieved from  
643 <https://nbn-resolving.org/urn:nbn:de:bsz:ch1-qucosa2-356553>

644 Beuth, F., & Hamker, F. H. (2015). A mechanistic cortical microcircuit of attention for amplification,  
645 normalization and suppression. *Vision Research*, *116*, 241-257. doi: <https://doi.org/10.1016/j.visres.2015>  
646 .04.004

647 Bicanski, A., & Burgess, N. (2018). A neural-level model of spatial memory and imagery. *eLife*, *7*, e33752.  
648 doi: <https://doi.org/10.7554/eLife.33752>

649 Bicanski, A., & Burgess, N. (2020). Neuronal vector coding in spatial cognition. *Nature reviews. Neuroscience*,  
650 *21*(9), 453-470. doi: <https://doi.org/10.1038/s41583-020-0336-9>

651 Bisley, J. W., & Goldberg, M. E. (2003). Neuronal activity in the lateral intraparietal area and spatial  
652 attention. *Science*, *299*(5603), 81-86. doi: <https://doi.org/10.1126/science.1077395>

653 Bisley, J. W., & Mirpour, K. (2019). The neural instantiation of a priority map. *Current Opinion in*  
654 *Psychology*, *29*, 108-112. doi: <https://doi.org/10.1016/j.copsyc.2019.01.002>

655 Burgess, N. (2008). Spatial cognition and the brain. *Annals of the New York Academy of Sciences*, *1124*,  
656 77-97. doi: <https://doi.org/10.1196/annals.1440.002>

657 Byrne, P., Becker, S., & Burgess, N. (2007). Remembering the past and imagining the future: A neural model  
658 of spatial memory and imagery. *Psychological Review*, *114*(2), 340-375. doi: [https://doi.org/10.1037/](https://doi.org/10.1037/0033-295X.114.2.340)  
659 0033-295X.114.2.340

660 Cabeza, R., Ciaramelli, E., Olson, I. R., & Moscovitch, M. (2008). The parietal cortex and episodic memory:  
661 an attentional account. *Nature reviews. Neuroscience*, *9*(8), 613-625. doi: <https://doi.org/10.1038/nrn2459>

662 Carrasco, M. (2011). Visual attention: The past 25 years. *Vision Research*, *51*(13), 1484-1525. (Vision  
663 Research 50th Anniversary Issue: Part 2) doi: <https://doi.org/10.1016/j.visres.2011.04.012>

664 Cavanagh, P. (2011). Visual cognition. *Vision Research*, *51*(13), 1538-1551. (Vision Research 50th Anniversary  
665 Issue: Part 2) doi: <https://doi.org/10.1016/j.visres.2011.01.015>

666 Colby, C., & Goldberg, M. (1999). Space and attention in parietal cortex. *Annual Review of Neuroscience*,  
667 *22*, 319-349. doi: <https://doi.org/10.1146/annurev.neuro.22.1.319>

668 Connor, C. E., & Knierim, J. J. (2017). Integration of objects and space in perception and memory. *Nature*  
669 *Neuroscience*, *20*(11), 1493-1503. doi: <https://doi.org/10.1038/nn.4657>

670 Desimone, R., & Duncan, J. (1995). Neural mechanisms of selective visual attention. *Annual Review of*  
671 *Neuroscience*, *18*, 193-222. doi: <https://doi.org/10.1146/annurev.ne.18.030195.001205>

672 Deubel, H., Schneider, W. X., & Bridgeman, B. (1996). Postsaccadic target blanking prevents saccadic  
673 suppression of image displacement. *Vision Research*, *36*(7), 985-996. doi: [https://doi.org/10.1016/](https://doi.org/10.1016/0042-6989(95)00203-0)  
674 0042-6989(95)00203-0

- 675 Drewes, J., Feder, S., & Einhäuser, W. (2021). Gaze during locomotion in virtual reality and the real world.  
676 *Frontiers in Neuroscience*, *15*, 656913. doi: <https://doi.org/10.3389/fnins.2021.656913>
- 677 Eliasmith, C., Stewart, T. C., Choo, X., Bekolay, T., Dewolf, T., Tang, Y., & Rasmussen, D. (2012). A  
678 Large-Scale Model of the Functioning Brain. *Science*, *338*, 1202-1205. doi: <https://doi.org/10.1126/science.1225266>  
679
- 680 Epstein, R. A., Patai, E. Z., Julian, J. B., & Spiers, H. J. (2017). The cognitive map in humans: spatial  
681 navigation and beyond. *Nature Neuroscience*, *20*, 1504-1513. doi: <https://doi.org/10.1038/nn.4656>
- 682 Gegenfurtner, K. R., & Kiper, D. C. (2003). Color vision. *Annual Review of Neuroscience*, *26*(1), 181-206.  
683 doi: <https://doi.org/10.1146/annurev.neuro.26.041002.131116>
- 684 Goldberg, M. E., Bisley, J. W., Powell, K. D., & Gottlieb, J. (2006). Chapter 10 saccades, salience and  
685 attention: the role of the lateral intraparietal area in visual behavior. In S. Martinez-Conde, S. Macknik,  
686 L. Martinez, J.-M. Alonso, & P. Tse (Eds.), *Visual perception* (Vol. 155, p. 157-175). Elsevier. doi:  
687 [https://doi.org/10.1016/S0079-6123\(06\)55010-1](https://doi.org/10.1016/S0079-6123(06)55010-1)
- 688 Golomb, J. D., Pulido, V. Z., Albrecht, A. R., Chun, M. M., & Mazer, J. A. (2010). Robustness of the retinotopic  
689 attentional trace after eye movements. *Journal of Vision*, *10*(3). doi: <https://doi.org/10.1167/10.3.19>
- 690 Gottlieb, J. (2007). From thought to action: The parietal cortex as a bridge between perception, action, and  
691 cognition. *Neuron*, *53*(1), 9-16. doi: <https://doi.org/10.1016/j.neuron.2006.12.009>
- 692 Hamker, F. H. (2003). The reentry hypothesis: linking eye movements to visual perception. *Journal of Vision*,  
693 *3*(14), 808-816. doi: <https://doi.org/10.1167/3.11.14>
- 694 Hamker, F. H. (2005a). The emergence of attention by population-based inference and its role in distributed  
695 processing and cognitive control of vision. *Computer Vision and Image Understanding*, *100*(1), 64-  
696 106. (Special Issue on Attention and Performance in Computer Vision) doi: <https://doi.org/10.1016/j.cviu.2004.09.005>  
697
- 698 Hamker, F. H. (2005b). The reentry hypothesis: The putative interaction of the frontal eye field, ventrolateral  
699 prefrontal cortex, and areas v4, it for attention and eye movement. *Cerebral Cortex*, *15*(4), 431-447. doi:  
700 <https://doi.org/10.1093/cercor/bhh146>
- 701 Hamker, F. H. (2015). Spatial Cognition of Humans and Brain-inspired Artificial Agents. *KI - Künstliche*  
702 *Intelligenz*, *29*, 83-88. doi: <https://doi.org/10.1007/s13218-014-0338-8>
- 703 Hamker, F. H., Zirnsak, M., Calow, D., & Lappe, M. (2008). The peri-saccadic perception of objects and  
704 space. *PLOS Computational Biology*, *4*(2). doi: <https://doi.org/10.1371/journal.pcbi.0040031>

705 Hollingworth, A. (2007). Object-position binding in visual memory for natural scenes and object arrays.  
706 *Journal of Experimental Psychology: Human Perception and Performance*, 33(1), 31. doi: [https://doi.org/](https://doi.org/10.1037/0096-1523.33.1.31)  
707 10.1037/0096-1523.33.1.31

708 Jamalain, A., Bergelt, J., Dinkelbach, H. U., & Hamker, F. H. (2017). Spatial attention improves object  
709 localization: A biologically plausible neuro-computational model for use in virtual reality. *2017 IEEE*  
710 *International Conference on Computer Vision Workshops*. doi: <https://doi.org/10.1109/iccvw.2017.320>

711 Jamalain, A., Beuth, F., & Hamker, F. H. (2016). The performance of a biologically plausible model of visual  
712 attention to localize objects in a virtual reality. In *International Conference on Artificial Neural Networks*  
713 *- ICANN 2016, Lecture Notes in Computer Science 9887* (pp. 447–454). doi: [https://doi.org/10.1007/](https://doi.org/10.1007/978-3-319-44781-0_53)  
714 978-3-319-44781-0\_53

715 Jones, J. P., & Palmer, L. A. (1987). An evaluation of the two-dimensional Gabor filter model of simple  
716 receptive fields in cat striate cortex. *Journal of Neurophysiology*, 58(6), 1233-1258. doi: [https://doi.org/](https://doi.org/10.1152/jn.1987.58.6.1233)  
717 10.1152/jn.1987.58.6.1233

718 Jonikaitis, D., Szinte, M., Rolfs, M., & Cavanagh, P. (2013). Allocation of attention across saccades. *Journal*  
719 *of Neurophysiology*, 109(5), 1425-34. doi: <https://doi.org/10.1152/jn.00656.2012>

720 Konkle, T., Brady, T. F., Alvarez, G. A., & Oliva, A. (2010). Scene memory is more detailed than you  
721 think: The role of categories in visual long-term memory. *Psychological Science*, 21(11), 1551-1556. doi:  
722 <https://doi.org/10.1177/0956797610385359>

723 Land, M. F. (2009). Vision, eye movements, and natural behavior. *Visual neuroscience*, 26(1), 51-62. doi:  
724 <https://doi.org/10.1017/s0952523808080899>

725 Lian, Y., Williams, S., Alexander, A. S., Hasselmo, M. E., & Burkitt, A. N. (2023). Learning the vector  
726 coding of egocentric boundary cells from visual data. *Journal of Neuroscience*. doi: [https://doi.org/10.1523/](https://doi.org/10.1523/JNEUROSCI.1071-22.2023)  
727 JNEUROSCI.1071-22.2023

728 Logothetis, N. K., Pauls, J., & Poggio, T. (1995). Shape representation in the inferior temporal cortex of  
729 monkeys. *Current Biology*, 5(5), 552-563. doi: [https://doi.org/10.1016/s0960-9822\(95\)00108-4](https://doi.org/10.1016/s0960-9822(95)00108-4)

730 Lu, J., Behbahani, A. H., Hamburg, L., Westeinde, E. A., Dawson, P. M., Lyu, C., Maimon, G., Dickinson,  
731 M. H., Druckmann, S., & Wilson, R. I. (2022). Transforming representations of movement from body- to  
732 world-centric space. *Nature*, 601, 98–104. doi: <https://doi.org/10.1038/s41586-021-04191-x>

733 Maith, O., Schwarz, A., & Hamker, F. H. (2021). Optimal attention tuning in a neuro-computational  
734 model of the visual cortex–basal ganglia–prefrontal cortex loop. *Neural Networks*, 142, 534–547. doi:  
735 <https://doi.org/10.1016/j.neunet.2021.07.008>



- 736 Milner, D., & Goodale, M. (1995). *The Visual Brain in Action*. Oxford University Press. doi: [https://doi.org/](https://doi.org/10.1093/acprof:oso/9780198524724.001.0001)  
737 10.1093/acprof:oso/9780198524724.001.0001
- 738 Mishkin, M., Ungerleider, L. G., & Macko, K. A. (1983). Object vision and spatial vision: two cortical  
739 pathways. *Trends in Neurosciences*, 6, 414-417. doi: [https://doi.org/10.1016/0166-2236\(83\)90190-X](https://doi.org/10.1016/0166-2236(83)90190-X)
- 740 Moulin-Frier, C., Fischer, T., Petit, M., Pointeau, G., Puigbo, J., Pattacini, U., Low, S. C., Camilleri, D.,  
741 Nguyen, P., Hoffmann, M., Chang, H. J., Zambelli, M., Mealier, A., Damianou, A., Metta, G., Prescott,  
742 T. J., Demiris, Y., Dominey, P. F., & Verschure, P. F. M. J. (2018). Dac-h3: A proactive robot cognitive  
743 architecture to acquire and express knowledge about the world and the self. *IEEE Transactions on Cognitive*  
744 *and Developmental Systems*, 10(4), 1005-1022. doi: <https://doi.org/10.1109/TCDS.2017.2754143>
- 745 Navalpakkam, V., & Itti, L. (2007). Search goal tunes visual features optimally. *Neuron*, 53(4), 605–617. doi:  
746 <https://doi.org/10.1016/j.neuron.2007.01.018>
- 747 Novin, S., Fallah, A., Rashidi, S., Beuth, F., & Hamker, F. H. (2021). A neuro-computational model of  
748 visual attention with multiple attentional control sets. *Vision Research*, 189, 104-118. doi: [https://doi.org/](https://doi.org/10.1016/j.visres.2021.08.009)  
749 10.1016/j.visres.2021.08.009
- 750 O’Keefe, J., & Burgess, N. (1996). Geometric determinants of the place fields of hippocampal neurons. *Nature*,  
751 381, 425-428. doi: <https://doi.org/10.1038/381425a0>
- 752 Pouget, A., Deneve, S., & Duhamel, J. R. (2002). A computational perspective on the neural basis of  
753 multisensory spatial representations. *Nature Reviews Neuroscience*, 3(9), 741-747. doi: [https://doi.org/](https://doi.org/10.1038/nrn914)  
754 10.1038/nrn914
- 755 Pouget, A., & Sejnowski, T. J. (1997). Spatial Transformations in the Parietal Cortex Using Basis Functions.  
756 *Journal of Cognitive Neuroscience*, 9(2), 222-237. doi: <https://doi.org/10.1162/jocn.1997.9.2.222>
- 757 Rolfs, M., Jonikaitis, D., Deubel, H., & Cavanagh, P. (2010). Predictive remapping of attention across eye  
758 movements. *Nature Neuroscience*, 14(2), 252-259. doi: <https://doi.org/10.1038/nn.2711>
- 759 Salsano, I., Santangelo, V., & Macaluso, E. (2021). The lateral intraparietal sulcus takes viewpoint changes  
760 into account during memory-guided attention in natural scenes. *Brain Structure and Function*, 226,  
761 989–1006. doi: <https://doi.org/10.1007/s00429-021-02221-y>
- 762 Schall, J., Thompson, K., Bichot, N., Murthy, A., & Sato, T. (2004). Visual processing in the macaque  
763 frontal eye field. In C. E. C. Jon H. Kaas (Ed.), *The primate visual system* (p. 205-230). CRC Press. doi:  
764 <https://doi.org/10.1201/9780203507599>
- 765 Sestieri, C., Shulman, G. L., & Corbetta, M. (2017). The contribution of the human posterior parietal cortex to  
766 episodic memory. *Nature reviews. Neuroscience*, 18(3), 183-192. doi: <https://doi.org/10.1038/nrn.2017.6>

767 Smith Breault, M. (2020). Monkey brain. *Zenodo*. Retrieved from <https://doi.org/10.5281/zenodo>  
768 .3926117

769 Summerfield, J. J., Lepsien, J., Gitelman, D. R., Mesulam, M. M., & Nobre, A. C. (2006). Orienting  
770 attention based on long-term memory experience. *Neuron*, *49*(6), 905-916. doi: <https://doi.org/10.1016/>  
771 [j.neuron.2006.01.021](https://doi.org/10.1016/j.neuron.2006.01.021)

772 Teichmann, M., Larisch, R., & Hamker, F. H. (2021). Performance of biologically grounded models of  
773 the early visual system on standard object recognition tasks. *Neural Networks*, *144*, 210-228. doi:  
774 <https://doi.org/10.1016/j.neunet.2021.08.009>

775 Treue, S. (2001). Neural correlates of attention in primate visual cortex. *Trends in Neurosciences*, *24*(5),  
776 295-300. doi: [https://doi.org/10.1016/S0166-2236\(00\)01814-2](https://doi.org/10.1016/S0166-2236(00)01814-2)

777 Van Wetter, S. M., & Van Opstal, A. J. (2008). Experimental test of visuomotor updating models that  
778 explain perisaccadic mislocalization. *Journal of Vision*, *8*(14). doi: <https://doi.org/10.1167/8.14.8>

779 Vitay, J., Dinkelbach, H., & Hamker, F. H. (2015). Annarchy: a code generation approach to neural  
780 simulations on parallel hardware. *Frontiers in Neuroinformatics*, *9*, 19. Retrieved from <https://doi.org/>  
781 [10.5281/zenodo.6417924](https://doi.org/10.5281/zenodo.6417924) doi: <https://doi.org/10.3389/fninf.2015.00019>

782 Whitlock, J. R., Sutherland, R. J., Witter, M. P., Moser, M.-B., & Moser, E. I. (2008). Navigating from  
783 hippocampus to parietal cortex. *Proceedings of the National Academy of Sciences of the United States of*  
784 *America*, *105*(39), 14755-14762. doi: <https://doi.org/10.1073/pnas.0804216105>

785 Ziesche, A., Bergelt, J., Deubel, H., & Hamker, F. H. (2017). Pre- and post-saccadic stimulus timing in  
786 saccadic suppression of displacement – a computational model. *Vision Research*, *138*. doi: <https://doi.org/>  
787 [10.1016/j.visres.2017.06.007](https://doi.org/10.1016/j.visres.2017.06.007)

788 Ziesche, A., & Hamker, F. H. (2011). A computational model for the influence of corollary discharge and  
789 proprioception on the perisaccadic mislocalization of briefly presented stimuli in complete darkness. *Journal*  
790 *of Neuroscience*, *31*(48), 17392-17405. doi: <https://doi.org/10.1523/JNEUROSCI.3407-11.2011>

791 Ziesche, A., & Hamker, F. H. (2014). Brain circuits underlying visual stability across eye movements -  
792 converging evidence for a neuro-computational model of area lip. *Frontiers in Computational Neuroscience*,  
793 *8*, 25. doi: <https://doi.org/10.3389/fncom.2014.00025>

794 Zirnsak, M., Beuth, F., & Hamker, F. H. (2011). Split of spatial attention as predicted by a systems-level  
795 model of visual attention. *European Journal of Neuroscience*, *33*(11), 2035-2045. doi: <https://doi.org/>  
796 [10.1111/j.1460-9568.2011.07718.x](https://doi.org/10.1111/j.1460-9568.2011.07718.x)